Dalton Transactions

Accepted Manuscript

ROYAL SOCIETY OF CHEMISTRY

www.rsc.org/dalton

Fluoride-free Hiyama Coupling by Palladium Abnormal N-heterocyclic Carbene Complexes

Sudipta Modak,† Manoj Kumar Gangwar,† Mitta Nageswar Rao,† Madasu Mahesh,† Alok Ch. Kalita,† Vincent Dorcet,‡ Mayuri Arun Shejale,† Ray J. Butcher¶ and Prasenjit Ghosh*,†

†Department of Chemistry,
Indian Institute of Technology Bombay,
Powai, Mumbai 400 076.

‡Université de Rennes 1,
Institut des Sciences chimiques de Rennes,
Campus de Beaulieu, 35042 – Rennes, France

¶ Department of Chemistry
Howard University.
Washington DC 20059, USA

Email: pghosh@chem.iitb.ac.in

Fax: +91-22-2572-3480

Abstract: A series of palladium complexes of the abnormal N-heterocyclic carbene ligands of the type (*a*-NHC)PdI_2(L) [L = NC_5H_5 (**1**−**3**)**b** and PPh_3 (**1**−**3**)**c**] effectively catalyzed the Hiyama coupling of aryl bromides and iodides with $PhSi(OMe)_3$ under the much desired fluoride-free conditions. Interestingly enough, the pyridine based *trans*-(**1**−**3**)**b** complexes and a PPh_3 derived *cis*-**3c** complex exhibited higher yields than the related PPh_3 derived *trans*-(**1**−**2**)**c** complexes. The superior performances of the pyridine based *trans*-(**1**−**3**)**b** complexes and the PPh_3 derived *cis*-**3c** complex have been correlated to a tighter binding of the *a*-NHC ligand to the palladium center in these complexes leading to a greater (*a*-NHC) ligand influence on the metal center partaking the catalysis.

Introduction

Recent reports of the superior performances of some abnormal N-heterocyclic carbene catalysts over their much-explored normal N-heterocyclic carbene counterparts in reactions like, Suzuki coupling[1, 2] and hydrogenation,[3, 4] have aroused considerable interest on these ligands.[5] The abnormal N-Heterocyclic carbenes by virtue of the carbenic center being flanked by one electronegative heteroatom are more electron rich than the normal N-heterocyclic carbenes, in which the carbenic center is located between two electronegative heteroatoms.[6, 7] More importantly, in many instances, much of the observed higher catalytic activities of the abnormal N-Heterocyclic carbene complexes have been attributed to the electron richness of these ligands.[8-10]

With one of our key objectives being in the development of the N-heterocyclic carbene chemistry from the perspectives of their utility in homogeneous catalysis and biomedical applications,[11-13] we remain committed to studying the various scaffolds of the normal and abnormal N-heterocyclic carbene ligands for the promises they hold. In this context, we have recently reported the catalytic utility of the palladium complexes of the abnormal N-heterocyclic carbenes derived from N-fused heterocycles[14, 15] in the much-preferred Cu-free and the amine-free Sonogashira coupling reaction in air. Continuing further along the line, we decided to study their utility in another potentially important but relatively unexplored C-C cross-coupling reaction, namely the Hiyama coupling between an aryl halide and an organosilicon nucleophile.[16, 17]

The recent emphasis on the Hiyama coupling stems from the viable alternative it offers to the much-popular Suzuki coupling arising from the use of non-toxic and inexpensive organosilicon reagent as the organic nucleophile. It enjoys certain advantages over other potential rival alternatives like the Stille coupling, which suffers from toxicity issues associated with the use of organotin reagents.[18, 19] However, despite its promise and also unlike the Suzuki coupling, which has been extensively studied with the N-heterocyclic carbene based catalysts, the Hiyama coupling has remained relatively unexplored. Till date, only a handful of examples of the Hiyama coupling by the N-heterocyclic carbene based catalysts have been reported.[20-23]

Towards this goal, our specific objective was in developing the PEPPSI-themed (Pyridine Enhanced Precatalyst Preparation Stabilization and Initiation)[24-26] (*a*-NHC)$PdX_2(NC_5H_5)$ (X = halide) type precatalysts of the abnormal N-heterocyclic carbene ligands for the Hiyama coupling. The justification of our effort arises not only from the absence of any such report of abnormal N-heterocyclic carbene based catalysts for the Hiyama coupling but also for the continuation of our earlier effort on the utility of the PEPPSI themed palladium precatalysts of the more ubiquitous normal N-heterocyclic carbene ligands for the fluoride-free Hiyama coupling[23] and the Suzuki coupling.[27] We speculated that the abnormal N-heterocyclic carbene being more electron rich might perform better in the C-C cross-coupling reaction, and stretching the concept further, we decided to study the even more electron rich mixed abnormal N-heterocyclic carbene/phosphine based precatalysts of the type (*a*-NHC)$PdX_2(PPh_3)$ (X = halide) for the Hiyama coupling. It must be noted that

some mixed phosphine/NHC complexes have been reported to exhibit superior performances in certain catalysis.[28-32]

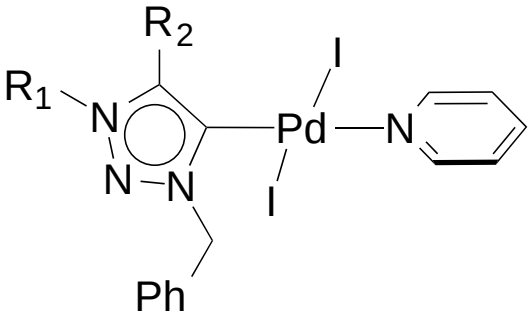

R_1 = Me, R_2 = $C_6H_{10}OH$ (**1b**)
R_1 = Et, R_2 = $C_6H_{10}OH$ (**2b**)
R_1 = Me, R_2 = Ph (**3b**)

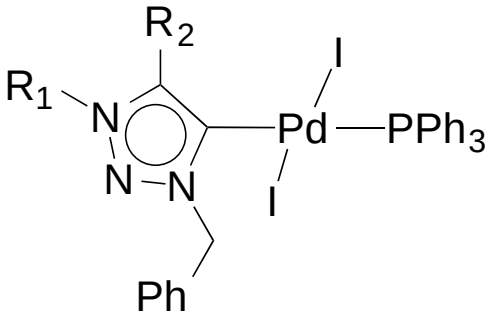

R_1 = Me, R_2 = $C_6H_{10}OH$ (**1c**)
R_1 = Et, R_2 = $C_6H_{10}OH$ (**2c**)

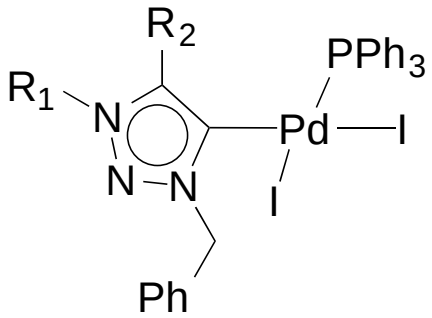

R_1 = Me, R_2 = Ph (**3c**)

Figure 1.

Here in the manuscript, we report a series of abnormal N-heterocyclic carbene based palladium precatalysts of the type (*a*-NHC)PdI_2(L) [L = NC_5H_5 (**1**−**3**)**b** and PPh_3 (**1**−**3**)**c**] for the fluoride-free Hiyama coupling performed in the presence of NaOH as a base under aerobic conditions.

Results and Discussions

The three 1,2,3-triazole derived abnormal N-heterocyclic carbene ligands namely, {(1-benzyl-3-R_1-4-R_2-1,2,3-triazol-5-ylidene} (R_1 = Me, Et; R_2 = $C_6H_{10}OH$, Ph) were obtained from the corresponding 1,2,3-triazole derivatives by the direct alkylation reactions with the methyl and ethyl iodide reagents (Scheme 1). The formation of the 1,2,3-triazolium iodide salts (**1**−**3**)**a** were evident from the observation of the characteristic carbene resonances at 8.90−9.23 ppm in the ^{1}H NMR spectrum of these compounds. Furthermore, the reaction of (**1**−**3**)**a** with $PdCl_2$ in pyridine in the presence of an excess of KI and K_2CO_3 as a base yielded the pyridine bound (*a*-NHC)$PdI_2(NC_5H_5)$ type complexes (**1**−**3**)**b**. Finally, with the anticipation that the mixed phosphine/NHC complexes might exhibit superior catalytic activity,[28-32] the mixed phosphine/(*a*-NHC) derivatives of the type (*a*-NHC)$PdI_2(PPh_3)$ (**1**−**3**)**c** were conveniently prepared by the treatment of the pyridine derived (**1**−**3**)**b** complexes with PPh_3 in *ca*. 70−78 % yields.

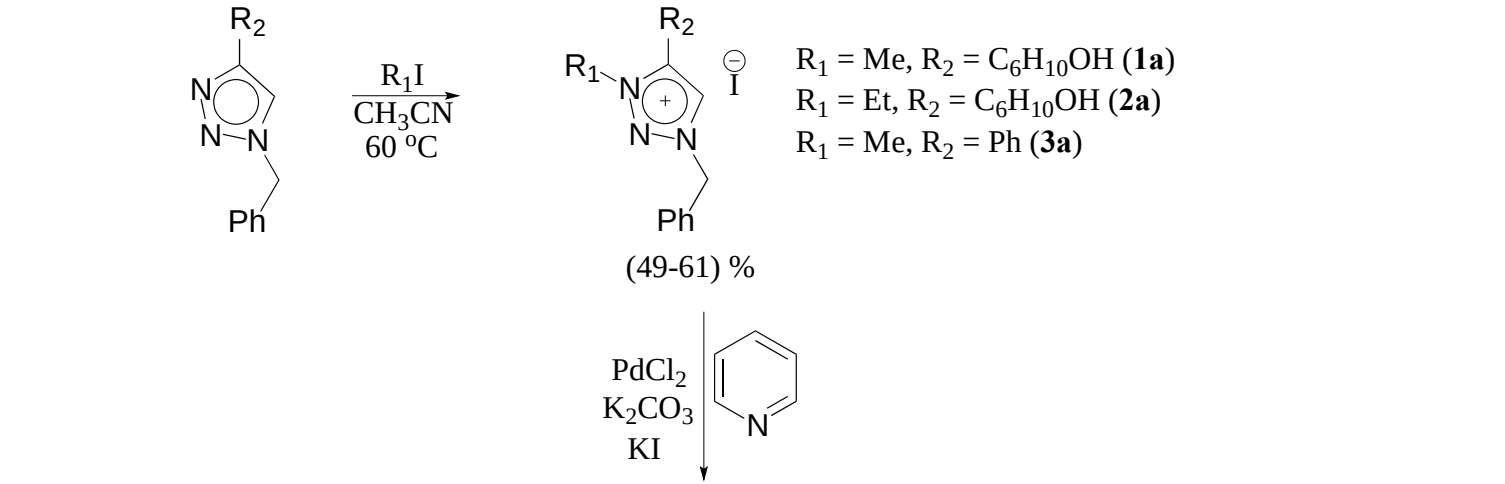

Scheme 1.

Quite interestingly, the $^{31}P\{^{1}H\}$ NMR spectrum of (**1**−**3**)**c** indicated the formation of the *trans*-isomers in case of the (**1**−**2**)**c** complexes and a *cis*-isomer in case of the **3c** complex, as evidenced from the appearance of the characteristic Pd−$\underline{P}Ph_3$ resonance at 16.9−17.0 ppm for the (**1**−**2**)**c** complexes and at 25.2 ppm for the **3c** complex, and which are in concurrence with the related ones known in the literature (Supporting Information Tables S1 and S2). The, final validation of the $^{31}P\{^{1}H\}$ NMR results came from the X-ray diffraction studies (Figures 2−4 and the Supporting Information Figures S50, S57 and S63 and Tables S22−S23) that confirmed the *trans* geometry for the (**1**−**2**)**c** complexes and a *cis* geometry for the **3c** complex. It is worth noting that for the (NHC)$PdI_2(PR_3)$ type of the mixed phosphine/NHC complexes, different geometrical isomers have been isolated depending upon the sterics and the electronic demands of the N-heterocyclic carbene and the phosphine ligands used for the stabilization of these complexes (Supporting Information Tables S1 and S2). In this context, the density functional theory study, undertaken at the B3LYP/SDD, 6-31G(d) level of theory, revealed that the *trans*-isomer was more stable by 15.8−4.2 kcal/mol than the *cis*-isomer for all of the pyridine based (**1**−**3**)**b** complexes and the phosphine based (**1**−**3**)**c** complexes (Supporting Information Figure S11). Notably, higher relative energy difference between the *cis*-and the *trans*-isomers were observed for the pyridine based (**1**−**3**)**b** complexes (15.8−13.1 kcal/mol) than for the phosphine based (**1**−**3**)**c** complexes (4.6−4.2 kcal/mol). Consistent with these DFT results, the *trans*-isomers were isolated for all [(**1**−**3**)**b** and (**1**−**2**)**c** complexes] but one case. The only instance, for which the *cis*-isomer was obtained, was for a phosphine based complex (**3c**) having the lowest relative energy difference between the *cis*-and the *trans*-forms of 4.2 kcal/mol among these pairs of the *cis*/*trans*-complexes.

Of significant interest are the Pd−$C_{carbene}$ bond distances as they provide useful insight on the nature of the chemical bond (Figures 2−4, Supporting Information S50, S57 and S63, Tables S22−23). In this regard, the significantly shorter Pd−$C_{carbene}$ bond distances of [1.967(3)−1.986(5)] Å in the pyridine based (**1**−**3**)**b** complexes in comparison to that of [2.006(6)−2.047(5)] Å in the phosphine based (**1**−**3**)**c** complexes, is suggestive of a stronger Pd−$C_{carbene}$ bonding interaction in the former. Furthermore, among the phosphine based (**1**−**3**)**c** complexes, the Pd−$C_{carbene}$ bond distance is shorter in the *cis*-**3c** complex [2.006(6) Å] than in the *trans*-(**1**−**2**)**c** complexes [2.047(5)−2.042(3) Å]. Consistent with the observed correlation, the Pd−$C_{carbene}$ bond dissociation energy (D_e) of the pyridine based (**1**−**3**)**b** complexes (80.9−81.4 kcal/mol) were indeed higher than that of the phosphine based (**1**−**3**)**c** complexes (64.8−64.9 kcal/mol), as estimated at the B3LYP/SDD, 6-31G(d) level of theory (Figure 5 and Supporting Information Figures S1). It is worth noting that the Pd−$C_{carbene}$ bonding interaction reflects directly on the NHC influence that the ligand exerts on the metal center of these complexes, and which in turn affects the catalysis as would be seen later.

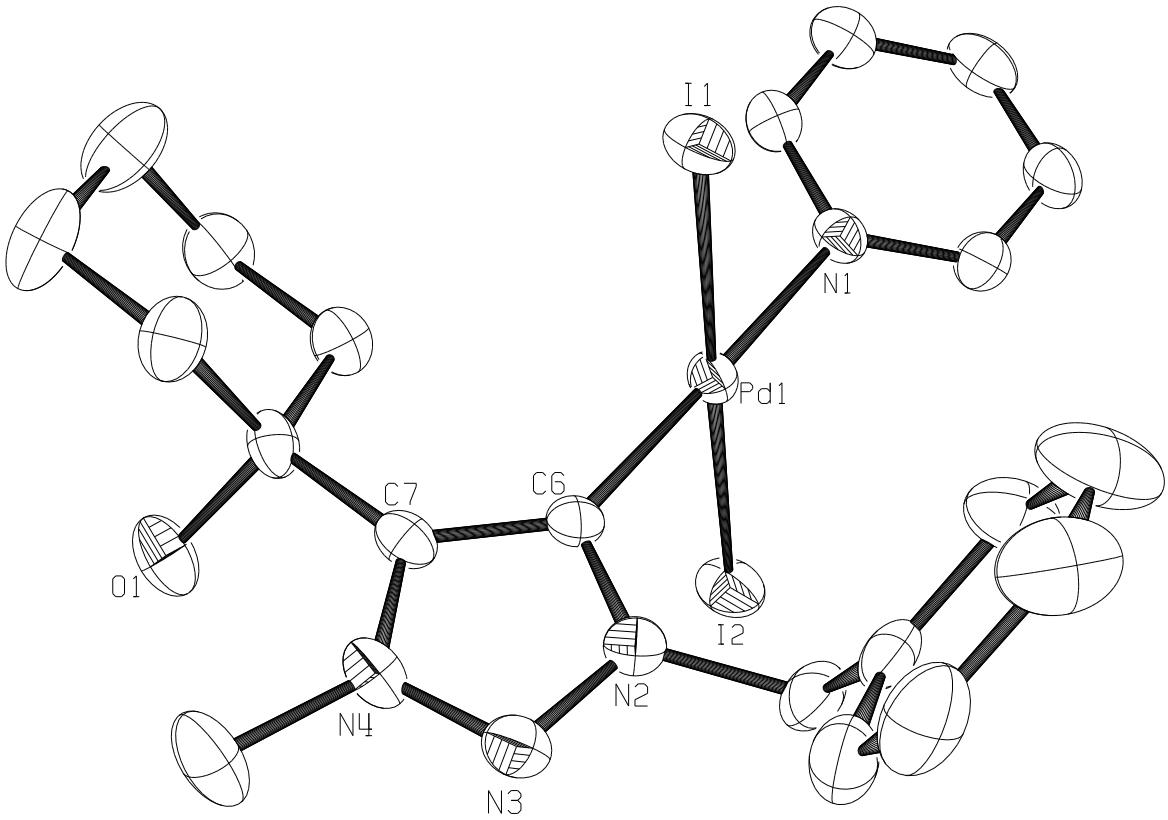

Figure 2. ORTEP diagram of **1b** with thermal ellipsoids shown at the 50 % probability level. Selected bond lengths (Å) and angles (°): Pd(1)-C(6) 1.980(3), Pd(1)-N(1) 2.091(3), Pd(1)-I(1) 2.6152(6), Pd(1)-I(2) 2.6135(6), C(6)-Pd(1)-N(1) 178.27(13), C(6)-Pd(1)-I(1) 89.93(9), N(1)-Pd(1)-I(1) 90.27(8), C(6)-Pd(1)-I(2) 88.95(9), N(1)-Pd(1)-I(2) 90.92(8), I(2)-Pd(1)-I(1) 177.550(15).

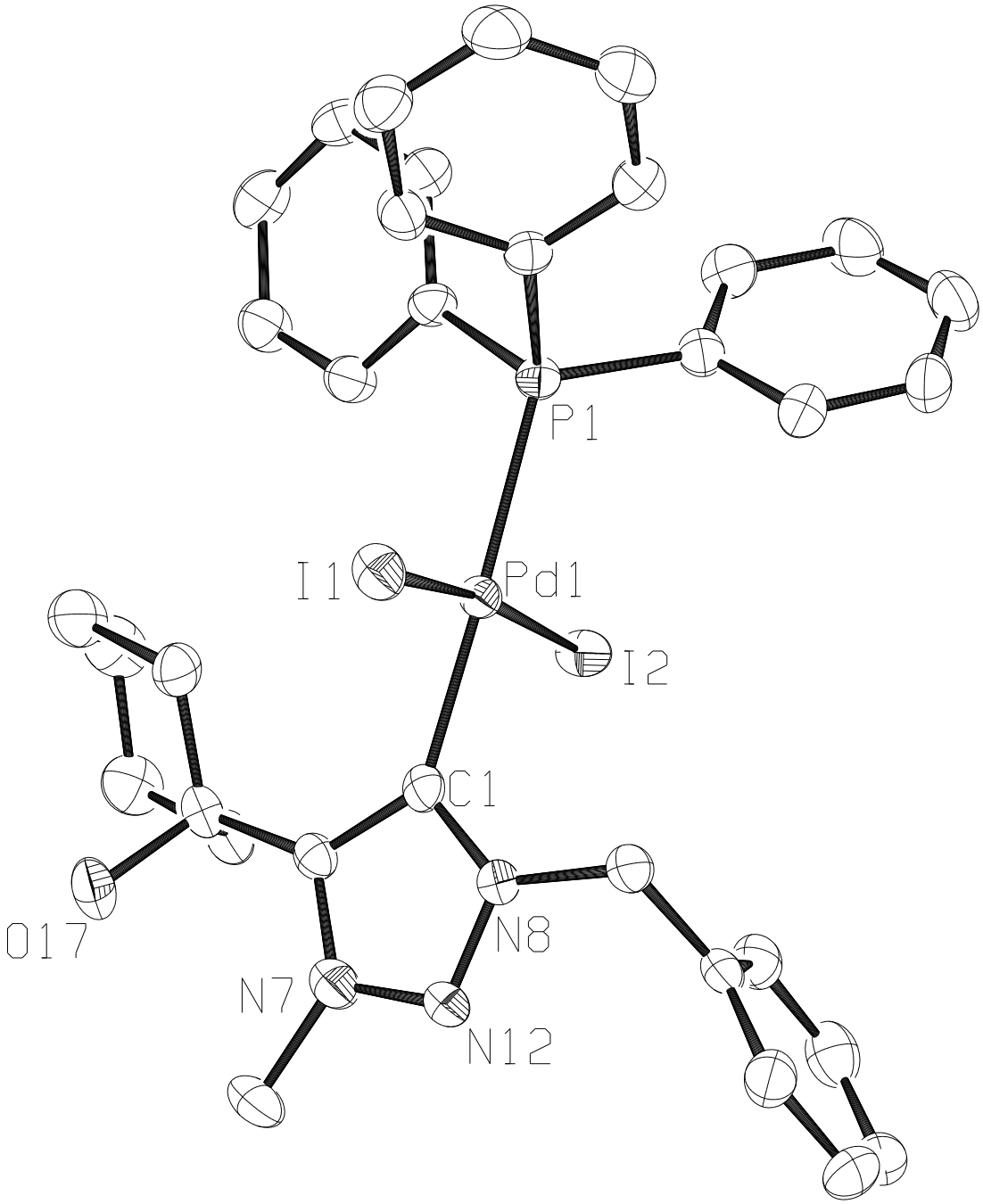

Figure 3. ORTEP diagram of **1c** with thermal ellipsoids shown at the 50 % probability level. Selected bond lengths (Å) and angles (°): Pd(1)-C(1) 2.047(5), Pd(1)-P(1) 2.3571(13), Pd(1)-I(2) 2.6145(7), Pd(1)-I(1) 2.5998(7), C(1)-Pd(1)-P(1) 176.80(14), C(1)-Pd(1)-I(2) 88.10(13), P(1)-Pd(1)-I(2) 90.42(4), C(1)-Pd(1)-I(1) 84.96(13), P(1)-Pd(1)-I(1) 96.76(4), I(1)-Pd(1)-I(2) 171.484(19).

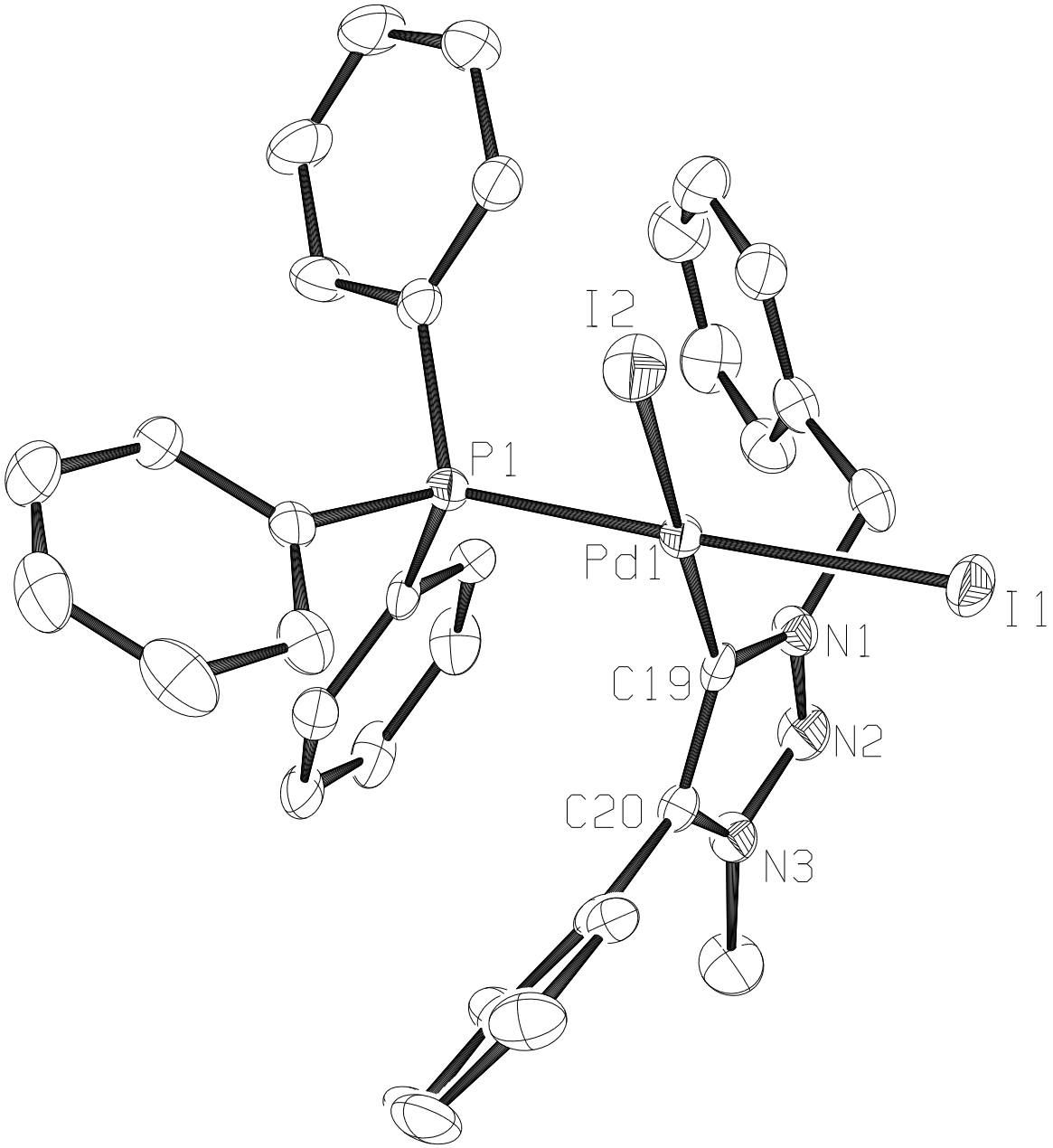

Figure 4. ORTEP diagram of **3c** with thermal ellipsoids shown at the 50 % probability level. Selected bond lengths (Å) and angles (°): Pd(1)-C(19) 2.006(6), Pd(1)-P(1) 2.2804(17), Pd(1)-I(2) 2.6399(12), Pd(1)-I(1) 2.6546(9), C(19)-Pd(1)-P(1) 91.41(17), C(19)-Pd(1)-I(2) 174.76(18), P(1)-Pd(1)-I(2) 91.69(4), C(19)-Pd(1)-I(1) 86.36(16), P(1)-Pd(1)-I(1) 175.88(5), I(2)-Pd(1)-I(1) 90.79(2).

A key design component of our *trans*-(*a*-NHC)PdI_2(L) type complexes [L = NC_5H_5 (**1**−**3**)**b** and PPh_3 (**1**−**2**)**c**], is the "L" ligand, that is located *trans* to the NHC ligand. The "L" ligand is conveniently referred to as a "throwaway" ligand owing to its weaker binding to the metal center that arise out of a stronger σ-binding of the *trans*-NHC ligand to the metal center. The concept was elaborately developed by Organ[24, 25, 33-35] in the form of the PEPPSI themed complexes that serve as effective catalysts for many C−C cross-coupling reactions.

From this particular perspective, the Pd−L (L = NC_5H_5, PPh_3) bond distances in the *trans*-(*a*-NHC)PdI_2(L) type complexes (L = NC_5H_5, PPh_3), (**1**−**3**)**b** and (**1**−**2**)**c**, are of considerable interest. In particular, the Pd−L distances of [2.091(3)−2.104(2)] Å observed in the pyridine based (**1**−**3**)**b** complexes and of [2.3515(9)−2.3571(13)] Å in the phosphine based (**1**−**2**)**c** complexes are shorter than the sum of the respective individual covalent radii [*d*(Pd−N) = 2.10 Å and *d*(Pd−P) = 2.46 Å] (Figures 2−4 and the Supporting Information Figures S50, S57 and S63 and Tables S22−S23).[36] Consistent with the "throwaway" attribute of the "L" ligand (L = NC_5H_5, PPh_3) in these complexes, the Pd−L (L = NC_5H_5, PPh_3) bond dissociation energy (D_e) of the pyridine based (**1**−**3**)**b** complexes (30.3−30.5 kcal/mol) and the phosphine based *trans*-(**1**−**2**)**c** complexes (32.7 kcal/mol) along with its *cis*-**3c** (37.9 kcal/mol) complex are significantly lower than the $Pd-C_{carbene}$ bond dissociation energy (D_e) of the pyridine based (**1**−**3**)**b** complexes (80.9−81.4 kcal/mol) and the phosphine based (**1**−**3**)**c** complexes (64.8−64.9 kcal/mol), as computed at the B3LYP/SDD, 6-31G(d) level of theory (Supporting Information Tables S3−S4). Also noteworthy is the fact that the $Pd-N_{pyridine}$ bond dissociation energies (D_e) of the pyridine based (**1**−**3**)**b** complexes (30.3−30.5 kcal/mol) are slightly lower than the $Pd-P_{phosphine}$ bond

dissociation energies (D_e) of the phosphine based (**1**−**3**)**c** complexes (32.7−37.9 kcal/mol), thus suggesting that pyridine is a better throwaway ligand than PPh_3 in these complexes (Supporting Information Tables S5−S6). The success of the *trans*-(NHC)PdI_2(L) type complexes as catalysts is very much dependent on the ease with which the "L" ligand makes way for the incoming substrate during catalysis, and in line with which, we decided to carryout a comparative study of the pyridine based (**1**−**3**)**b** complexes and the phosphine based (**1**−**2**)**c** complexes and also a *cis*-**3c** complex for their utility in the fluoride-free Hiyama coupling.

Further understanding of the Pd−$C_{carbene}$ and the Pd−L (L = NC_5H_5, PPh_3) interactions in the (**1**−**3**)**b** and (**1**−**3**)**c** complexes were obtained by constructing the corresponding molecular orbital (MO) correlation diagrams from the individual fragment molecular orbitals (FMOs) of the constituting components (Figures 5 and 6 and Supporting Information Figures S1−S10). A scrutiny of these molecular orbital correlation diagram reveals that the Pd−$C_{carbene}$ molecular orbital (MO) is composed of the individual fragment molecular orbitals (FMOs) of the (*a*-NHC) fragment and the $PdI_2(NC_5H_5)$ fragment in case of the pyridine based (**1**−**3**)**b** complexes (Figure 5 and Supporting Information Figure S1−S2) and of the (*a*-NHC) fragment and the $PdI_2(PPh_3)$ fragment for the phosphine based (**1**−**3**)**c** complexes (Supporting Information Figure S3−S5). Along the same line, the molecular orbitals for the Pd−$N_{pyridine}$ σ-interactions were composed of the fragment molecular orbitals (FMOs) of the (*a*-NHC)PdI_2 fragment and the (NC_5H_5) fragment for the pyridine based (**1**−**3**)**b** complexes (Figure 6 and Supporting Information Figure S6−S7) while the Pd−$P_{phosphine}$ σ-interactions were comprised of the fragment molecular orbitals

(FMOs) of the (*a*-NHC)PdI_2 fragment and the (PPh_3) fragment for the phosphine based (**1**−**3**)**c** complexes (Supporting Information Figure S8−S10).

A closer look at these molecular orbital correlation diagrams further indicates that in the Pd−$C_{carbene}$ σ-interactions in these *trans*-(*a*-NHC)PdI_2(L) [L = NC_5H_5, PPh_3] type complexes, (**1**−**3**)**b** and (**1**−**2**)**c**, the electron donation occurs from the $C_{carbene}$ lone pair of the *a*-NHC ligand on to the σ*-orbital of the Pd−L (L = NC_5H_5, PPh_3) bond of the PdI_2L fragments (Figure 5 and Supporting Information Figures S1−S5). Likewise, for the Pd−$N_{pyridine}$ and the Pd−$P_{phosphine}$ σ-interactions in the *trans*-(*a*-NHC)PdI_2(L) [L = NC_5H_5, PPh_3] type complexes, (**1**−**3**)**b** and (**1**−**2**)**c**, the electron donation takes from the N-(pyridine) lone pair on to the σ*-orbital of the Pd−$C_{carbene}$ bond of the (*a*-NHC)PdI_2 fragment in the pyridine based (**1**−**3**)**b** complexes and from the P-(PPh_3) lone pair on to the σ*-orbital of the Pd−$C_{carbene}$ bond of the (*a*-NHC)PdI_2 fragment in the phosphine based (**1**−**2**)**c** complexes (Figure 6 and Supporting Information Figures S6−S9).

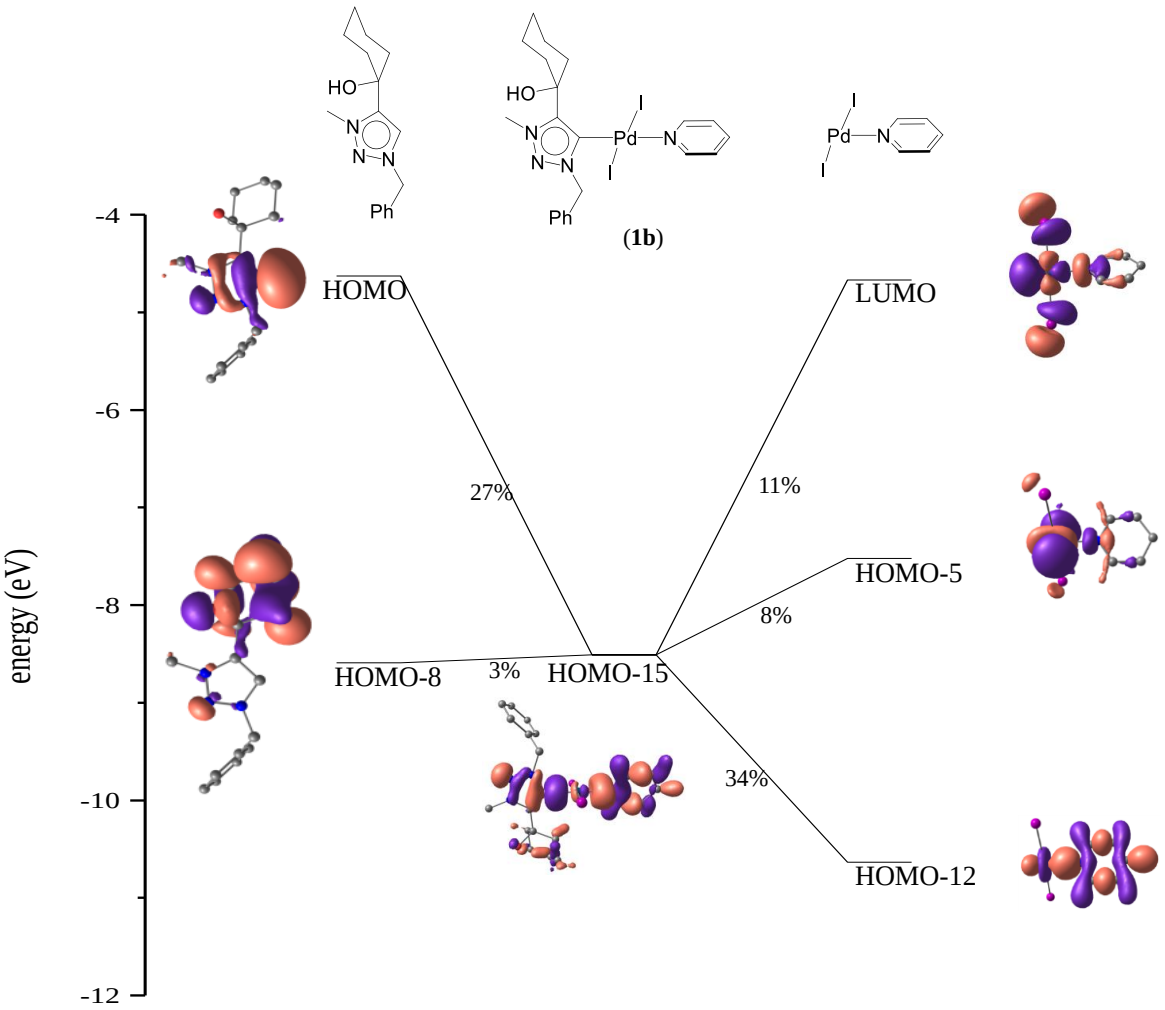

Figure 5. Simplified orbital interaction diagram showing major contribution to the (*a*-NHC)–Pd bonding orbital HOMO-15 in **1b**.

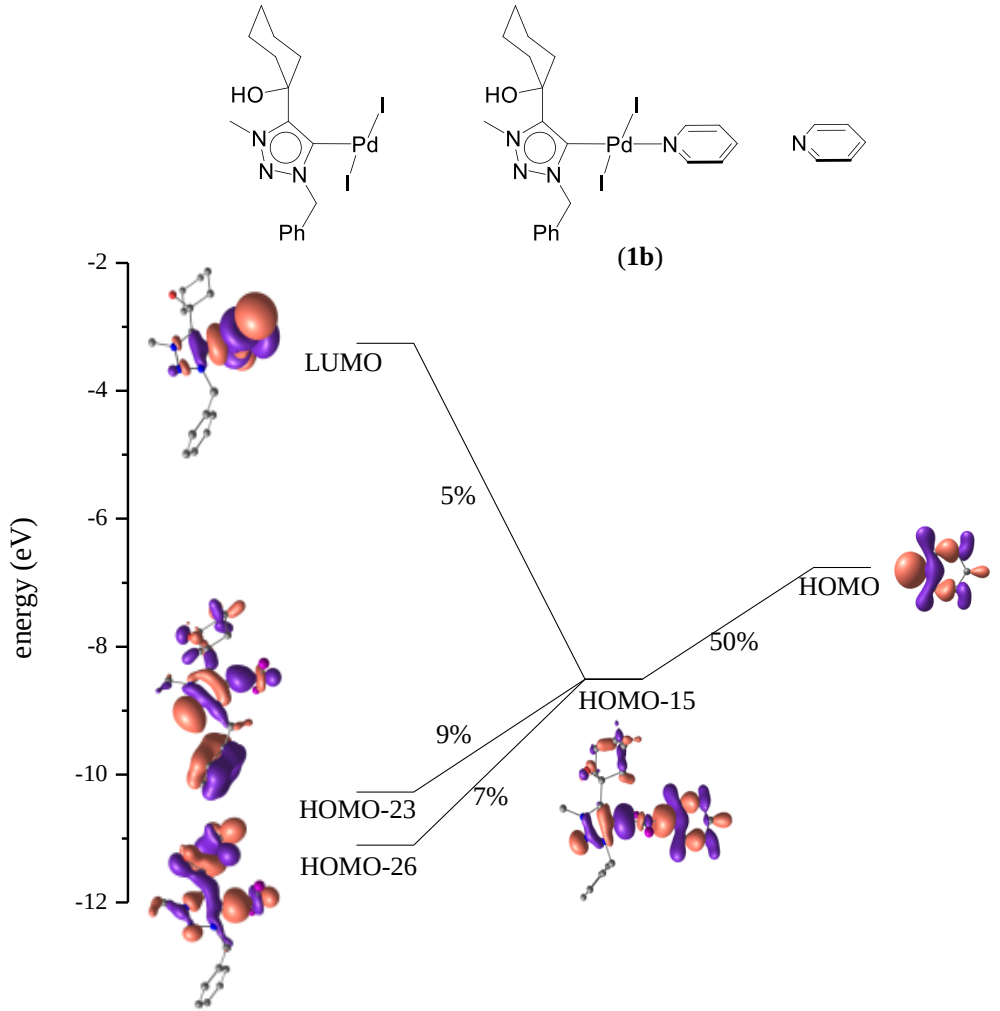

Figure 6. Simplified orbital interaction diagram showing major contribution to the Pd–NC_5H_5 bonding orbitals in **1b**.

Likewise, for the structurally different *cis*-**3c** complex, the molecular orbital for the Pd−$C_{carbene}$ σ-interaction represented electron donation from the $C_{carbene}$ lone pair on to the σ*-orbital of the *trans*-Pd−I bond of the $PdI_2(PPh_3)$ fragment while the molecular orbital for the Pd−$P_{phosphine}$ σ-interaction indicated electron donation from the P-(PPh_3) lone pair on to the σ*-orbital of the *trans*-Pd−I bond of the (*a*-NHC)$PdI_2(PPh_3)$ fragment (Supporting Information Figures S5 and S10).

A Natural Bond Orbital (NBO) analysis showed that the Pd−$C_{carbene}$ bond in the pyridine based (**1**−**3**)**b** complexes is less polar with 68.9−69.2 % electron contribution from the $C_{carbene}$ atom and 30.8−31.1 % electron contribution from the Pd atom than that of the phosphine based (**1**−**3**)**c** complexes with 75.5−76.3 % electron contribution from the $C_{carbene}$ atom and 23.7−24.4 % electron contribution from the Pd atom (Supporting Information Table S20). The difference in the polarity of the Pd−$C_{carbene}$ bond between the pyridine based (**1**−**3**)**b** and the phosphine based (**1**−**3**)**c** complexes would reflect on the catalytic activity of these complexes as encountered later during the catalysis study.

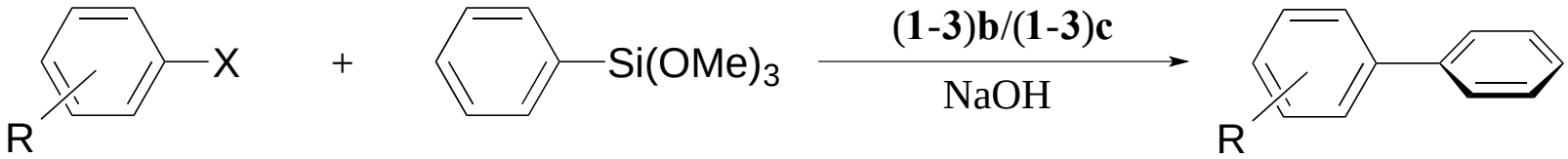

R = H, Me, $COCH_3$, NO_2
X = Br, I

Equation 1.

Quite significantly, both of the pyridine based (**1**−**3**)**b** complexes and the phosphine based (**1**−**3**)**c** complexes successfully carried out the much-preferred fluoride-free Hiyama coupling of the aryl bromide and the iodide substrate with an organosilicon reagent giving the desired biaryl product (Equation 1 and Table 1). Specifically, the Hiyama coupled products were seen for various aryl halide substrates ranging from the activated ones namely the, 4'-bromoacetophenone, 4-bromonitrobenzene, 1-bromo-2-nitrobenzene and 2'-bromoacetophenone to the inactivated ones like, iodobenzene and 4-iodotoluene. The solvent optimization study yielded the maximum conversion in a mixed medium of dioxane and water (2:1, v/v) (Supporting Information Table S36) while the variation of base produced the best result with NaOH (Supporting Information Table S37). After varying the catalyst stoichiometry, the 2 mol % of the catalyst loading was chosen for the subsequent runs undertaken for the catalysis study (Supporting Information Table S38).

Table 1. Selected results for Hiyama cross-coupling reaction of aryl halides (ArX; X = I, Br) catalyzed by (**1**–**3**)**b** and (**1**–**3**)**c**.

entry	reagent	Reagent	cross-coupled product	yields[a] (**1b**)	(**1c**)	(**2b**)	(**2c**)	(**3b**)	(**3c**)
1	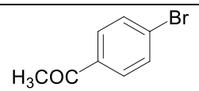	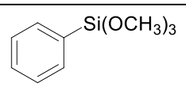	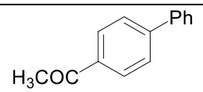	96	65	82	68	78	97
2	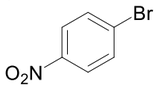	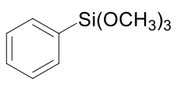	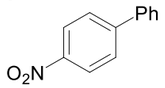	75	70	88	89	93	95
3	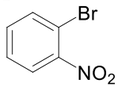	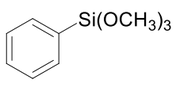	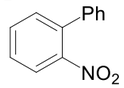	21	23	28	24	63	84
4	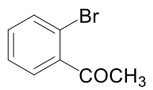	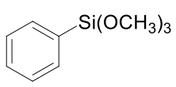	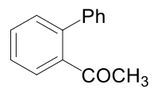	41	36	33	25	66	78
5		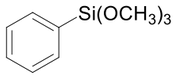	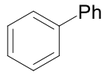	94	82	91	81	75	82
6	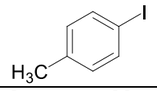	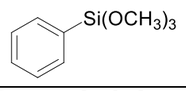	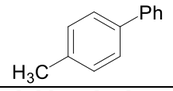	63	57	61	49	60	62

[a] The yields (%) were determined by GC using diethylene glycol dibutyl ether as an internal standard. Reaction conditions: 1.00 mmol of aryl halides, 1.20 mmol of $PhSi(OMe)_3$, 1.00 mmol of diethylene glycol dibutyl ether, 3.00 mmol of NaOH, 2 mol% of catalyst (**1**–**3**)**b**, (**1**–**3**)**c** and 6 mL of 1,4-dioxane/H_2O (2:1), at 80 °C for 4 hours.

Considerable ligand influence of the *a*-NHC ligand on the catalysis was very much evident from the amplification of the product yields of up to *ca*. 37 %, observed for the pyridine based (**1**−**3**)**b** and the phosphine based (**1**−**3**)**c** complexes relative to that of the control runs performed with $PdCl_2$ (Supporting Information Table S39). The time dependence profile of the of the coupling reaction for two representative substrates namely, 4-bromoacetophenone and $PhSi(OMe)_3$ as catalyzed by **3b** in the presence and absence of Hg, indicated some extent of catalyst degradation occurring in the presence of Hg resulting in comparatively lower catalysis yields ((Figures 7 and 8 and Supporting Information Table S39).[37] In these time dependence Hg drop experiments, the Hg additions were carried out at different time intervals after the start of the reaction with the product conversions recorded before each Hg additions and after the end of the catalysis run time of 4 hours (Figure 8). In this regard it is worth noting that similar type of catalyst degradation has been reported for related PEPPSI themed complexes.[38-40]

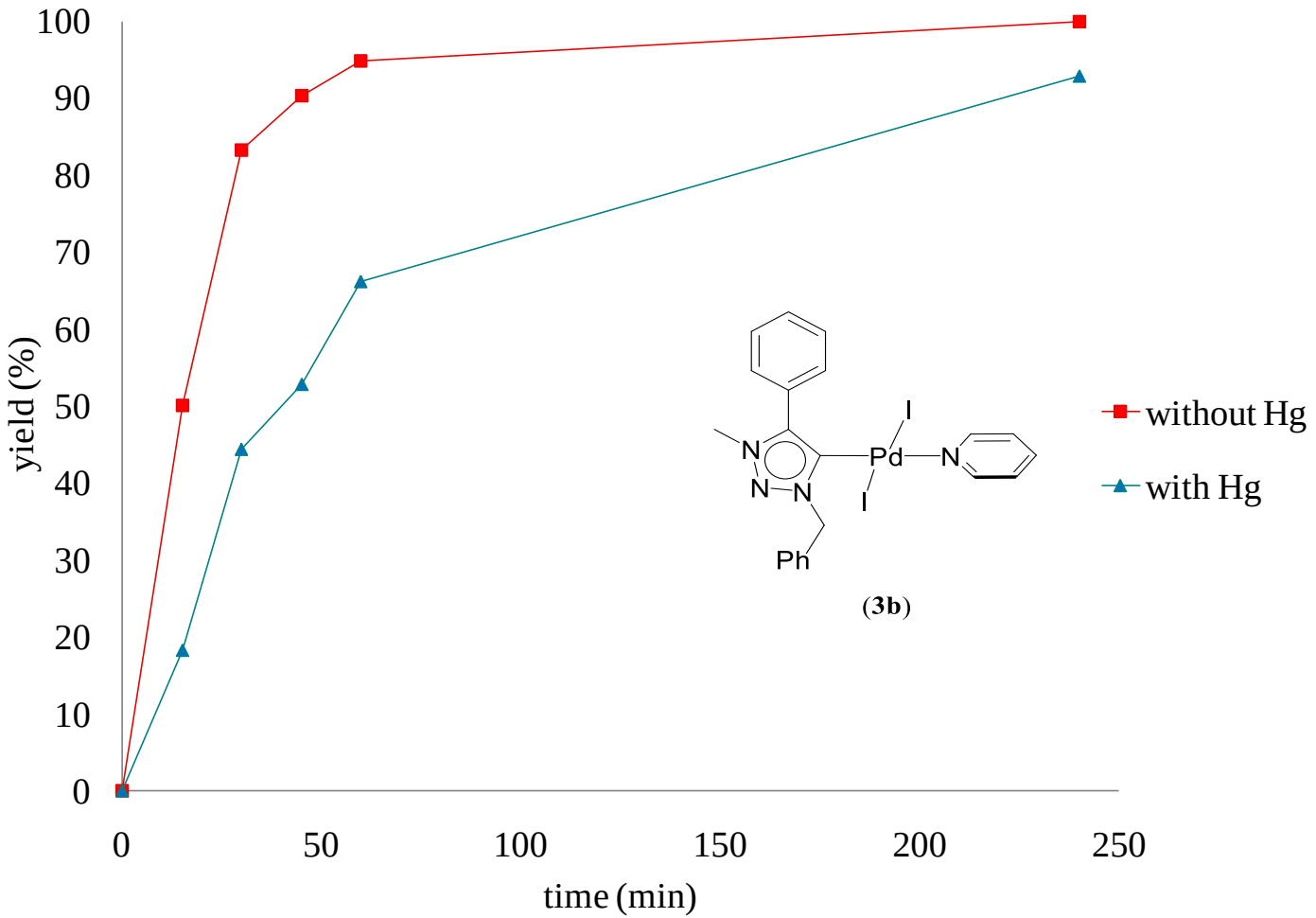

Figure 7. A time profile overlay of the Fluoride-free Hiyama coupling of 4-bromoacetophenone and $PhSi(OMe)_3$ as catalyzed by **3b** in the presence and absence of Hg.

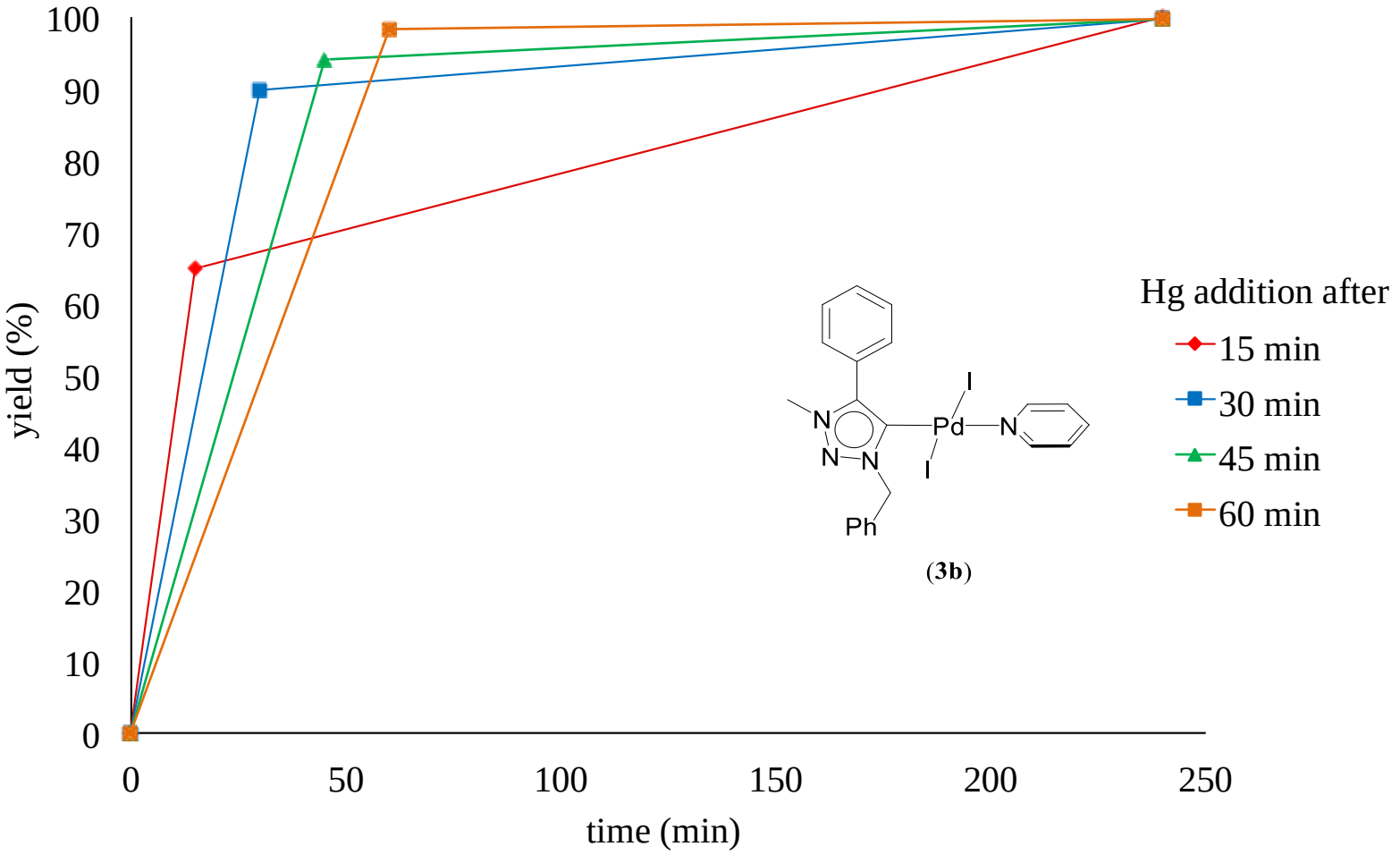

Figure 8. A time profile overlay of the fluoride-free Hiyama coupling of 4-bromoacetophenone and $PhSi(OMe)_3$ as catalyszed by **3b** as a function of Hg addition at varying time intervals.

Of foremost interest is the comparison of the catalysis results of the pyridine based (**1**−**3**)**b** complexes and the two types of the phosphine based *trans*-(**1**−**2**)**c** complexes and the *cis*-**3c** complex. Quite interestingly, the pyridine based (**1**−**3**)**b** complexes consistently exhibited higher yields than the phosphine based *trans*-(**1**−**2**)**c** complexes (Entries 1−6, Table 1), and this can be ascribed to a greater (*a*-NHC) ligand influence on catalysis arising from a stronger binding of the (*a*-NHC) ligand to the metal center in the pyridine based (**1**−**3**)**b** complexes. The explanation was substantiated by the X-ray diffraction studies that showed shorter Pd−$C_{carbene}$ bond distances in the pyridine based (**1**−**3**)**b** complexes [1.967(3)−1.986(5)] Å than in the phosphine based *trans*-(**1**−**2**)**c** complexes [2.042(3)−2.047(5)] Å (Figures 2−4, Supporting Information S50, S57 and S63, Tables S22−S23). Additionally, the density functional theory studies displayed higher Pd−$C_{carbene}$ bond dissociation energy (D_e) in the pyridine based (**1**−**3**)**b** complexes (80.9−81.4 kcal/mol) than the phosphine based *trans*-(**1**−**2**)**c** complexes (64.8−64.9 kcal/mol) (Supporting Information Tables S3−S4). In keeping with the above observation, the density functional theory studies also showed that the "pyridine" moiety was more labile as it exhibited a weaker Pd−$N_{pyridine}$ bond dissociation energy (D_e) in the pyridine based (**1**−**3**)**b** complexes (30.3−30.5 kcal/mol) than the corresponding Pd−$P_{phosphine}$ bond dissociation energy (D_e) of "PPh_3" moiety in the phosphine based *trans*-(**1**−**2**)**c** complexes (32.7 kcal/mol) (Supporting Information Tables S5−S6). All of these observations, thus, taken together, support the notion of a greater (*a*-NHC) ligand influence in the pyridine based (**1**−**3**)**b** complexes than that in the phosphine based *trans*-(**1**−**2**)**c** complexes, and which in the process account for the superior activity of the pyridine based (**1**−**3**)**b** complexes.

In this context it is worth mentioning that similar to our observation of superior performance of the NHC based percatalysts (**1**−**3**)**b** over the mixed phosphine/NHC counterparts, (**1**−**3**)**c**, in the fluoride-free Hiyama coupling, analogous higher activities of the hetero-*bis*(NHC) precatalysts over their mixed phosphine/NHC complexes have been noted for the Cu(I)-catalyzed azide−alkyne cycloaddition (CuAAC) reaction[41] and these are in contrast to the commonly observed better performances of the mixed phosphine/NHC complexes.[28-32]

Additionally, of particular interest is the observation that, among the phosphine based complexes, the *cis*-**3c** complex performed better than the *trans*-(**1**−**2**)**c** complexes, thereby indicating that the *cis*-geometry of the metal complex is more favorable for catalysis (Table 1). It is worth noting that the density functional theory studies, done at the B3LYP/SDD, 6-31G(d) level of theory, had shown earlier that the *cis*-isomer was more unstable than its *trans*-counterpart for all of the (**1**−**3**)**b** and (**1**−**3**)**c** complexes (Figure S11). In this context, it can thus be said that, though the catalytic performance of the *cis*-**3c** complex suggests that the *cis*-form is more promising for catalysis, the primary challenge would however lie on the isolation of these type of *cis*-complexes owing to their inherent instability relative to their *trans*-isomers. Lastly, the most active of all these catalyst, *i.e*. the *cis*-**3c** complex, however, failed to show much activity towards the more challenging aryl chloride substrates (Supporting Information Table S40).

Conclusions

In summary, a series of (*a*-NHC)PdI_2(L) [L = NC_5H_5, PPh_3] type complexes have been synthesized and structurally characterized. These complexes effectively

catalyzed the much-preferred fluoride-free Hiyama coupling of the aryl bromide and the iodide substrates with $PhSi(OMe)_3$ in presence of NaOH as a base. The pyridine based (**1**−**3**)**b** complexes exhibited superior activity than the phosphine based *trans*-(**1**−**2**)**c** complexes and thereby giving credence to the theory that a greater (*a*-NHC) ligand influence was evident in the former than in the latter. Though the catalysis results of the phosphine based *cis*-**3c** complex looked promising, the density functional theory study highlighted the challenges of the isolation of these types of the *cis*-complexes owing to their natural instability with regard to their *trans*-forms.

Experimental Section

General Procedures. All manipulations were carried out using standard Schlenk and glove box techniques. Solvents were purified and degassed by standard procedures. All starting precursors were purchased from Sigma-Aldrich and Spectrochem India and used without any further purification. ^{1}H, $^{13}C\{^{1}H\}$ and $^{31}P\{^{1}H\}$ NMR spectra were recorded on a Varian and Bruker 400 MHz NMR spectrometer. ^{1}H NMR peaks are labeled as singlet (s), doublet (d), triplet (t), quartet (q), doublet of doublets (dd), doublet of triplets (dt), triplet of triplets (tt), multiplet (m). The 1-(1-benzyl-1,2,3-triazol-4-yl)cyclohexanol,[42] 1-benzyl-3-methyl-4-phenyl-1,2,3-triazol-3-ium iodide[43] (**3a**) were synthesized by modification of procedures reported in literature. High resolution mass spectrometry measurements were done on a Micromass Q-Tof spectrometer and a Bruker maxis impact spectrometer. Infrared spectra were recorded on a Perkin Elmer Spectrum One FT-IR spectrometer. X-ray diffraction data for all compounds were collected on a Rigaku Hg 724+ diffractometer except for the compound **2c** for which the diffraction data was collected on APEXII, Bruker-AXS diffractometer equipped with a CCD detector and crystal data collection and refinement parameters are summarized in Tables S22–S23 (Supporting Information). The structures were solved using direct methods and standard difference map techniques, and were refined by full-matrix least-squares procedures on F^2 with SHELXTL.][44, 45] CCDC-922717 (**1b**), CCDC-935843 (**1c**), CCDC-926965 (**2b**), CCDC-926236 (**2c**), CCDC-934458 (**3b**), and CCDC-934462 (**3c**) contain the supplementary crystallographic data for this paper. These data can be obtained free of charge from the Cambridge Crystallographic Data center via www.ccdc.cam.ac.uk/data_request/cif. GC analyses were obtained on a PerkinElmer Clarus 600 equipped with a FID. All GC–MS analyses were done using Agilent

7890A GC system connected with 5975C inert XL EI/CI MSD (with triple axis detector). Elemental Analysis was carried out on Thermo Quest FLASH 1112 SERIES (CHNS) Elemental Analyzer.

Synthesis of 1-benzyl-4-(1-hydroxycyclohexyl)-3-methyl-1,2,3-triazol-3-ium iodide (1a)

A mixture of 1-(1-benzyl-1,2,3-triazol-4-yl)cyclohexanol (6.51 g, 25.3 mmol), and methyl iodide (17.9 g, 126 mmol) was stirred at 60 °C in CH_3CN (*ca.* 50 mL) for 24 hours, after which, the volatiles were removed under vacuum. The yellow solid thus obtained was further purified by column chromatography using silica gel as a stationary phase and eluted with a mixed medium of MeOH:CH_2Cl_2 (v/v 1:19) to give the product (**1a**) as a white solid (4.98 g, 49 %). ^{1}H NMR ($CDCl_3$, 400 MHz, 25 ^{o}C): δ 8.91 (s, 1H, $C_2\underline{H}N_3$), 7.61-7.59 (m, 2H, $C_6\underline{H}_5$), 7.43-7.40 (m, 3H, $C_6\underline{H}_5$), 5.85 (s, 2H, $C\underline{H}_2$), 4.48 (s, 1H, O$\underline{H}$), 4.44 (s, 3H, $C\underline{H}_3$), 2.21-1.21 (m, 10H, $C_6\underline{H}_{10}$). ^{13}C NMR ($CDCl_3$, 100 MHz, 25 ^{o}C): δ 149.7 ($\underline{C}_2HN_3$), 131.0 ($\underline{C}_6H_5$), 129.6 ($\underline{C}_6H_5$), 129.4 ($\underline{C}_6H_5$), 129.2 ($\underline{C}_6H_5$), 127.6 ($\underline{C}_2HN_3$), 68.5 ($\underline{C}_6H_{10}$), 56.9 ($\underline{C}H_2$), 41.2 ($\underline{C}H_3$), 36.7 ($\underline{C}_6H_{10}$), 24.4 ($\underline{C}_6H_{10}$), 20.6 ($\underline{C}_6H_{10}$). IR Data (KBr pellet) cm^{-1}: 3267 (s), 3067 (m), 2941 (m), 2855 (w), 1642 (w), 1496 (w), 1452 (w), 1341 (w), 1308 (w), 1260 (w), 1217 (w), 1163 (w), 1126 (w), 1083 (w), 990 (w), 905 (w), 861 (w), 737 (w), 700 (w), 640 (w), 597 (w). HRMS (ES): m/z 272.1759 $[M-I]^+$, calcd 272.1763. Anal. Calcd. for $C_{16}H_{22}IN_3O$: C, 48.13; H, 5.55; N, 10.52 Found: C, 48.41; H, 5.98; N, 9.99.

Synthesis of *trans*-{(1-benzyl-4-(1-hydroxycyclohexyl)-3-methyl-1,2,3-triazol-5-ylidene}$PdI_2(NC_5H_5)$ (1b)

A mixture of 1-benzyl-4-(1-hydroxycyclohexyl)-3-methyl-1,2,3-triazol-3-ium iodide (**1a**) (0.500 g, 1.25 mmol), $PdCl_2$ (0.222 g, 1.25 mmol), KI (1.04 g, 6.26 mmol) and K_2CO_3 (0.865 g, 6.26 mmol) was refluxed in pyridine (5 mL, 63 mmol) for 16 hours. The reaction mixture was cooled to room temperature, diluted with $CHCl_3$ (*ca.* 100 mL) and subsequently washed with saturated aqueous $CuSO_4$ solution (*ca.* 3 × 50 mL). The organic layer was separated and dried over anhydrous Na_2SO_4 and filtered. The filtrate was concentrated under vacuum to give a brown residue. The residue thus obtained was further purified by column chromatography using silica gel as a stationary phase and eluted with EtOAc: petroleum ether (1:4 *v*/*v*) to give the product **1b** as a bright orange solid (0.406 g, 46 %). Single crystals suitable for X-ray diffraction were obtained from THF by applying slow evaporation technique. ^{1}H NMR ($CDCl_3$, 400 MHz, 25 ^{o}C): δ 9.00 (dt, 2H, $^3J_{HH}$ = 5 Hz, $^4J_{HH}$ = 2 Hz, *o*-$NC_5\underline{H}_5$), 7.72 (tt, 1H, $^3J_{HH}$ = 8 Hz, $^4J_{HH}$ = 2 Hz, *p*-$NC_5\underline{H}_5$), 7.64 (dd, 2H, $^3J_{HH}$ = 8 Hz, $^4J_{HH}$ = 2 Hz, *m*-$NC_5\underline{H}_5$), 7.43-7.38 (m, 3H, $C_6\underline{H}_5$), 7.33-7.30 (m, 2H, $C_6\underline{H}_5$), 6.04 (s, 2H, $C\underline{H}_2$), 4.15 (s, 3H, $C\underline{H}_3$), 3.06-1.40 (m, 11H, $C_6\underline{H}_{10}$ & O$\underline{H}$). ^{13}C NMR ($CDCl_3$, 100 MHz, 25 ^{o}C): δ 154.2 (*o*-$N\underline{C}_5H_5$), 147.6 ($\underline{C}_2N_3$), 137.7 (*p*-$N\underline{C}_5H_5$), 133.6 ($\underline{C}_6H_5$), 130.5 ($\underline{C}_6H_5$), 130.1 ($\underline{C}_6H_5$), 129.0 ($\underline{C}_2N_3$), 128.9 ($\underline{C}_6H_5$), 124.7 (*m*-$N\underline{C}_5H_5$), 70.5 ($\underline{C}_6H_{10}$), 60.9 ($\underline{C}H_2$), 40.4 ($\underline{C}H_3$), 38.4 ($\underline{C}_6H_{10}$), 25.1 ($\underline{C}_6H_{10}$), 21.4 ($\underline{C}_6H_{10}$). IR Data (KBr pellet) cm^{-1}: 3447 (s), 2930 (s), 2853 (m), 1063 (m), 1496 (w), 1482 (w), 1445 (s), 1349 (w), 1327 (m), 1304 (w), 1254 (w), 1210 (m), 1148 (s), 1129 (m), 1082 (w), 1067 (m), 1037 (w), 972 (s), 903 (m), 852 (w), 759 (s)724 (m), 704 (s), 695 (s), 653 (m), 588 (w). HRMS (ES): m/z 376.0642 $[(NHC)Pd\text{-}H]^+$, calcd 376.0643. Anal. Calcd. for $C_{21}H_{26}I_2N_4OPd$: C, 35.49; H, 3.69; N, 7.88 Found: C, 35.35; H, 3.39; N, 7.48.

Synthesis of *trans*-{(1-benzyl-4-(1-hydroxycyclohexyl)-3-methyl-1,2,3-triazol-5-ylidene}$PdI_2(PPh_3)$ (1c)

A mixture of *trans*-{(1-methyl-2-(1-hydroxycyclohexyl)-4-benzyl-1,2,3-triazol-5-ylidene}$PdI_2(NC_5H_5)$ (**1b**) (0.135 g, 0.189 mmol) and PPh_3 (0.080 g, 0.305 mmol) in CH_2Cl_2 (*ca.* 30 mL) was stirred for 16 hours at room temperature. The solvent was evaporated under reduced pressure to give the crude orange solid which was further purified by column chromatography using silica gel as a stationary phase and eluted with a mixed medium of EtOAc:petroleum ether (v/v 1:4) to give the product (**1c**) as a light orange solid (0.130 g, 77 %). Single crystals suitable for X-ray diffraction were obtained from a mixture of C_2H_5OH and CH_2Cl_2 by applying slow evaporation technique. ^{1}H NMR ($CDCl_3$, 400 MHz, 25 ^{o}C): δ 7.77 – 7.39 (m, 20H, $4C_6\underline{H}_5$ from $P(\underline{C}_6H_5)_3$ & $CH_2\underline{C}_6H_5$), 5.88 (s, 2H, $C\underline{H}_2$), 4.18 (s, 3H, $C\underline{H}_3$), 2.83 – 1.27 (m, 11H, $C_6\underline{H}_{10}$ and $O\underline{H}$). ^{13}C NMR ($CDCl_3$, 100 MHz, 25 ^{o}C): δ 148.3 (d, $^2J_{CP}$ = 12 Hz, $\underline{C}_2N_3$), 143.2 ($\underline{C}_2N_3$), 141.4 ($\underline{C}_6H_5$), 135.3 (d, $^2J_{CP}$ = 11 Hz, $P(\underline{C}_6H_5)_3$), 133.6 ($\underline{C}_6H_5$), 133.2 ($\underline{C}_6H_5$), 132.7 ($\underline{C}_6H_5$), 130.3 (d, $^1J_{CP}$ = 12 Hz, $P(\underline{C}_6H_5)_3$), 128. 8 ($P(\underline{C}_6H_5)_3$), 127.9 (d, $^3J_{CP}$ = 10 Hz, $P(\underline{C}_6H_5)_3$), 70.4 ($\underline{C}_6H_{10}$), 60.4 ($\underline{C}H_2$), 39.9 ($\underline{C}H_3$), 38.4 ($\underline{C}_6H_{10}$), 25.1 ($\underline{C}_6H_{10}$), 21.4 ($\underline{C}_6H_{10}$). ^{31}P NMR ($CDCl_3$, 162 MHz, 25 ^{o}C): δ 17.0 ($\underline{P}Ph_3$). IR Data (KBr pellet) cm^{-1}: 3483 (s), 3059 (w), 2921 (s), 2855 (m), 1734 (w), 1635 (w), 1498 (w), 1478 (w), 1449 (w), 1433 (s), 1328 (w), 1286 (w), 1267 (w), 1240 (m), 1193 (w), 1147 (m), 1093 (m), 1072 (m), 1027 (w), 999 (w), 976 (m), 891 (m), 846 (w). 808 (w), 750 (m), 743 (m), 700 (s), 658 (w), 605 (w), 543 (w), 523 (s), 512 (m), 461 (w). HRMS (ES): m/z 766.0673 $[M-I]^+$, calcd 766.0676. Anal. Calcd. for $C_{34}H_{36}I_2N_3OPPd$: C, 45.69; H, 4.06; N, 4.70 Found: C, 45.07; H, 4.05; N, 5.66.

Synthesis of 1-benzyl-4-(1-hydroxycyclohexyl)-3-ethyl-1,2,3-triazol-3-ium iodide (2a)

A mixture of 1-(1-benzyl-1,2,3-triazol-4-yl)cyclohexanol (6.32 g, 24.6 mmol), and ethyl iodide (27.1 g, 173 mmol) was stirred for 24 hours at 60 °C in CH_3CN (*ca.* 50 mL), after which the volatiles were removed under vacuum. The slight yellow solid thus obtained was further purified by column chromatography using silica gel as a stationary phase and eluted with a mixed medium of MeOH:CH_2Cl_2 (v/v 1:19) to give the product (**2a**) as a white solid (6.23 g, 61 %). ^{1}H NMR ($CDCl_3$, 400 MHz, 25 ^{o}C): δ 8.90 (s, 1H, $C_2\underline{H}N_3$), 7.61-7.59 (m, 2H, $C_6\underline{H}_5$), 7.42-7.41 (m, 3H, $C_6\underline{H}_5$), 5.88 (s, 2H, $\underline{C}H_2$), 4.89 (q, 2H, $^3J_{HH}$ = 7 Hz, $C\underline{H}_2CH_3$), 4.61 (s, 1H, O$\underline{H}$), 2.21-1.17 (m, 10H, $C_6\underline{H}_{10}$), 1.66 (t, 3H, $^3J_{HH}$ = 7 Hz, $CH_2C\underline{H}_3$). ^{13}C NMR ($CDCl_3$, 100 MHz, 25 ^{o}C): δ 149.6 ($\underline{C}_2HN_3$), 131.0 ($\underline{C}_6H_5$), 129.5 ($\underline{C}_6H_5$), 129.2 ($\underline{C}_6H_5$), 129.1 ($\underline{C}_6H_5$), 127.2 ($\underline{C}_2HN_3$), 68.6 ($\underline{C}_6H_{10}$), 56.8 ($\underline{C}H_2$), 49.2 ($\underline{C}H_2$), 36.9 ($\underline{C}_6H_{10}$), 24.3 ($\underline{C}_6H_{10}$), 20.6 ($\underline{C}_6H_{10}$), 14.6 ($\underline{C}H_3$). IR Data (KBr pellet) cm^{-1}: 3265 (s), 3129 (w), 3075 (w), 2929 (s), 2860 (m), 1560 (m), 1497(w), 1452 (s), 1379 (w), 1351 (w), 1283 (m), 1264 (m), 1218 (w), 1193 (m), 1157 (s), 1136 (m), 1089 (w), 1065 (w), 1041 (w), 1025 (w), 995 (s), 944 (w), 907 (w), 894 (m), 834 (w), 737 (s), 704 (m), 662 (w), 632 (w), 608 (w), 505 (w), 461 (w). HRMS (ES): m/z 286.1933 $[M\text{-}I]^+$, calcd 286.1919. Anal. Calcd. for $C_{17}H_{24}IN_3O{\bullet}CH_3CN$: C, 50.23; H, 5.99; N, 12.33 Found: C, 50.28; H, 5.76; N, 12.68.

Synthesis of *trans*-{(1-benzyl-4-(1-hydroxycyclohexyl)-3-ethyl-1,2,3-triazol-5-ylidene}$PdI_2(NC_5H_5)$ (2b)

A mixture of 1-benzyl-4-(1-hydroxycyclohexyl)-3-ethyl-1,2,3-triazol-3-ium iodide (**2a**) (0.600 g, 1.45 mmol), $PdCl_2$ (0.257 g, 1.45 mmol), KI (1.20 g, 7.26 mmol) and

K_2CO_3 (1.00 g, 7.26 mmol) was refluxed in pyridine (5 mL, 63 mmol) for 16 hours. The reaction mixture was cooled to room temperature, diluted with $CHCl_3$ (*ca.* 100 mL) and subsequently washed with saturated aqueous $CuSO_4$ solution (*ca.* 3 × 50 mL). The organic layer was separated and dried over anhydrous Na_2SO_4 and filtered. The filtrate was concentrated under vacuum to give an yellow residue. The residue thus obtained was further purified by column chromatography using silica gel as a stationary phase and eluted with EtOAc: petroleum ether (1:4 *v*/*v*) to give the product **2b** as a bright orange solid (0.359 g, 34 %). Single crystals suitable for X-ray diffraction were obtained from THF by applying slow evaporation technique. ^{1}H NMR ($CDCl_3$, 400 MHz, 25 ^{o}C): δ 8.94 (dt, 2H, $^3J_{HH}$ = 5 Hz, $^4J_{HH}$ = 2 Hz, *o*-$NC_5\underline{H}_5$), 7.65 (tt, 1H, $^3J_{HH}$ = 8 Hz, $^4J_{HH}$ = 2 Hz, *p*-$NC_5\underline{H}_5$), 7.54 (dd, 2H, $^3J_{HH}$ = 8 Hz, $^4J_{HH}$ = 2 Hz, *m*-$NC_5\underline{H}_5$), 7.35-7.32 (m, 3H, $C_6\underline{H}_5$), 7.26-7.23 (m, 2H, $C_6\underline{H}_5$), 5.99 (s, 2H, $C\underline{H}_2$), 4.55 (q, 2H, $^3J_{HH}$ = 7 Hz, $C\underline{H}_2$), 3.03-0.81 (m, 11H, $C_6\underline{H}_{10}$ & OH), 1.40 (t, 3H, $^3J_{HH}$ = 7 Hz, $C\underline{H}_3$). ^{13}C NMR ($CDCl_3$, 100 MHz, 25 ^{o}C): δ 154.1 (*o*-$N\underline{C}_5H_5$), 147.5 ($\underline{C}_2N_3$), 137.6 (*p*-$N\underline{C}_5H_5$), 133.7 ($\underline{C}_6H_5$), 130.3 ($\underline{C}_6H_5$), 129.0 ($\underline{C}_6H_5$), 128.8 ($\underline{C}_2N_3$), 128.7 ($\underline{C}_6H_5$), 124.6 (*m*-$N\underline{C}_5H_5$), 70.5 ($\underline{C}_6H_{10}$), 60.9 ($\underline{C}H_2$), 48.3 ($\underline{C}H_2$), 38.8 ($\underline{C}_6H_{10}$), 25.1 ($\underline{C}_6H_{10}$), 21.4 ($\underline{C}_6H_{10}$), 15.5 ($\underline{C}H_3$). IR Data (KBr pellet) cm^{-1}: 3472 (s), 2921 (s), 2854 (m), 1733 (w), 1602 (w), 1446 (s), 1259 (w), 1212 (w), 1149 (m), 1071 (m), 1034 (m), 969 (m), 898 (w), 847 (w), 801 (w), 757 (w), 743 (w), 721 (w), 693 (s), 567 (w). HRMS (ES): m/z 390.0799 [(NHC)Pd-H]$^+$, calcd 390.0802. Anal. Calcd. for $C_{22}H_{28}I_2N_4OPd$: C, 36.46; H, 3.89; N, 7.73 Found: C, 36.75; H, 3.62; N, 8.59.

Synthesis of *trans*-{(1-benzyl-4-(1-hydroxycyclohexyl)-3-ethyl-1,2,3-triazol-5-ylidene}$PdI_2(PPh_3)$ (2c)

A mixture of *trans*-{(1-ethyl-2-(1-hydroxycyclohexyl)-4-benzyl-1,2,3-triazol-5-ylidene}$PdI_2(NC_5H_5)$ (**2b**) (0.171 g, 0.236 mmol) and PPh_3 (0.074 g, 0.282 mmol) was stirred in CH_2Cl_2 (*ca.* 30 mL) for 16 hours at room temperature, after which, the solvent was evaporated under reduced pressure to give the crude orange solid. The solid thus obtained was further purified by column chromatography using silica gel as a stationary phase and eluted with a mixed medium of EtOAc:petroleum ether (v/v 1:4) to give the product (**2c**) as a light orange solid (0.167 g, 78 %). Single crystals suitable for X-ray diffraction were obtained from CH_2Cl_2 by applying slow evaporation technique. ^{1}H NMR ($CDCl_3$, 400 MHz, 25 ^{o}C): δ 7.73 – 7.35 (m, 20 H, 4$C_6\underline{H}_5$ from P($\underline{C}_6H_5)_3$ & $CH_2\underline{C}_6H_5$), 5.87 (s, 2H, C$\underline{H}_2$), 4.61 (q, 2H, $^3J_{HH}$ = 7 Hz, C$\underline{H}_2$), 2.84 – 1.24 (m, 11H, $C_6\underline{H}_{10}$ & O$\underline{H}$), 1.46 (t, 3H, $^3J_{HH}$ = 7 Hz, C$\underline{H}_3$). ^{13}C NMR ($CDCl_3$, 100 MHz, 25 ^{o}C): δ 147.9 (d, $^2J_{CP}$ = 12 Hz, $\underline{C}_2N_3$), 142.4 ($\underline{C}_2N_3$), 140.5 ($\underline{C}_6H_5$), 135.1 (d, $^2J_{CP}$ = 10 Hz, P($\underline{C}_6H_5)_3$), 133.7 ($\underline{C}_6H_5$), 133.1 ($\underline{C}_6H_5$), 132.6 ($\underline{C}_6H_5$), 130.0 (P($\underline{C}_6H_5)_3$), 128.6 (d, $^1J_{CP}$ = 4 Hz, P($\underline{C}_6H_5)_3$), 127.7 (d, $^3J_{CP}$ = 10 Hz, P($\underline{C}_6H_5)_3$), 70.5 ($\underline{C}_6H_{10}$), 60.4 ($\underline{C}H_2$), 47.9 ($\underline{C}H_2$), 38.7 ($\underline{C}_6H_{10}$), 25.0 ($\underline{C}_6H_{10}$), 21.3 ($\underline{C}_6H_{10}$) 15.4 ($\underline{C}H_3$). ^{31}P NMR ($CDCl_3$, 162 MHz, 25 ^{o}C): δ 16.9 ($\underline{P}Ph_3$). IR Data (KBr pellet) cm^{-1}: 3854 (w), 3747 (w), 3484 (s), 3057 (w), 2921 (s), 2853 (m), 2343 (w), 1637 (w), 1478 (w), 1434 (m), 1262 (s), 1240 (w), 1147 (m), 1093 (s), 1026 (s), 889 (w), 804 (s), 749 (m), 701 (m), 691 (m), 524 (m). HRMS (ES): m/z 780.0865 $[M-I]^+$, calcd 780.0832. Anal. Calcd. for $C_{35}H_{38}I_2N_3OPPd$: C, 46.30; H, 4.22; N, 4.63. Found: C, 46.52; H, 3.71; N, 5.26.

Synthesis of *trans*-{(1-benzyl-3-methyl-4-phenyl-1,2,3-triazol-5-ylidene}$PdI_2(NC_5H_5)$ (3b)

A mixture of 1-benzyl-3-methyl-4-phenyl-1,2,3-triazol-3-ium iodide (**3a**) (0.650 g, 1.72 mmol), $PdCl_2$ (0.305 g, 1.72 mmol), KI (1.43 g, 8.61 mmol) and K_2CO_3 (1.19 g, 8.61 mmol) was refluxed in pyridine (5 mL, 63 mmol) for 16 hours. The reaction mixture was cooled to room temperature, diluted with $CHCl_3$ (*ca.* 100 mL) and subsequently washed with saturated aqueous $CuSO_4$ solution (*ca.* 3 × 50 mL). The organic layer was separated and dried over anhydrous Na_2SO_4 and filtered. The filtrate was concentrated under vacuum to give a sticky, yellow residue. The residue thus obtained was further purified by column chromatography using silica gel as a stationary phase and eluted with EtOAc: petroleum ether (1:4 *v*/*v*) to give the product **3b** as a yellow solid (0.548 g, 46 %). Single crystals suitable for X-ray diffraction were obtained from $CHCl_3$ by applying slow evaporation technique. ^{1}H NMR ($CDCl_3$, 400 MHz, 25 ^{o}C): δ 8.90 (dt, 2H, $^3J_{HH}$ = 4 Hz, $^4J_{HH}$ = 1 Hz, *o*-$NC_5\underline{H}_5$), 7.92 (dt, 2H, $^3J_{HH}$ = 6 Hz, $^4J_{HH}$ = 1 Hz, $C_6\underline{H}_5$), 7.72 (dd, 2H, $^3J_{HH}$ = 8 Hz, $^4J_{HH}$ = 2 Hz, $C_6\underline{H}_5$), 7.67 (tt, 1H, $^3J_{HH}$ = 8 Hz, $^4J_{HH}$ = 1 Hz, *p*-$NC_5\underline{H}_5$), 7.59-7.50 (m, 3H, $C_6\underline{H}_5$), 7.46-7.38 (m, 3H, $C_6\underline{H}_5$), 7.27-7.24 (m, 2H, *m*-$NC_5\underline{H}_5$), 6.04 (s, 2H, $C\underline{H}_2$), 3.92 (s, 3H, $C\underline{H}_3$). ^{13}C NMR ($CDCl_3$, 100 MHz, 25 ^{o}C): δ 153.8 (*o*-$N\underline{C}_5H_5$), 143.9 ($\underline{C}_2N_3$), 137.4 (*p*-$N\underline{C}_5H_5$), 134.6 ($\underline{C}_6H_5$), 133.5 ($\underline{C}_6H_5$), 130.5 ($\underline{C}_6H_5$), 130.3 ($\underline{C}_6H_5$), 129.9 ($\underline{C}_6H_5$), 128.9 ($\underline{C}_2N_3$), 128.8 ($\underline{C}_6H_5$), 128.7 ($\underline{C}_6H_5$), 127.4 ($\underline{C}_6H_5$), 124.3 (*m*-$N\underline{C}_5H_5$), 59.9 ($\underline{C}H_2$), 39.6 ($\underline{C}H_3$). IR Data (KBr pellet) cm^{-1}: 3433 (s), 2923 (m), 2852 (w), 1602 (m), 1446 (m), 1330 (w), 1279 (w), 1262 (w), 1239 (w), 1148 (w), 1070 (m), 1018 (m), 802 (w), 762 (m), 750 (m), 695 (s), 641 (w), 596 (w), 474 (w). HRMS (ES): m/z 481.9346 $[(NHC)PdI]^+$, calcd 481.9342. Anal. Calcd. for $C_{21}H_{20}I_2N_4Pd$: C, 36.63; H, 2.93; N, 8.14;. Found: C, 36.82; H, 2.67; N, 7.44.

Synthesis of *cis*-{(1-benzyl-3-methyl-4-phenyl-1,2,3-triazol-5-ylidene}$PdI_2(PPh_3)$ (3c)

A mixture of *trans*-{(1-methyl-2-phenyl-4-benzyl-1,2,3-triazol-5-ylidene}$PdI_2(NC_5H_5)$ (**3b**) (0.096 g, 0.139 mmol) and PPh_3 (0.069 g, 0.263 mmol) was stirred in CH_2Cl_2 (*ca.* 30 mL) for 16 hours at room temperature, after which, the solvent was evaporated under reduced pressure to give the crude yellow solid. The solid thus obtained was further purified by column chromatography using silica gel as a stationary phase and eluted with a mixed medium of $CHCl_3$:MeOH (v/v 9:1) to give the product (**3c**) as a bright yellow solid (0.085 g, 70 %). Single crystals suitable for X-ray diffraction were obtained from a mixture of CH_3CN and $CHCl_3$ by applying slow evaporation technique. ^{1}H NMR ($CDCl_3$, 400 MHz, 25 ^{o}C): δ 7.69 – 7.03 (m, 25H, 5$C_6\underline{H}_5$ from P($\underline{C}_6H_5$)$_3$ & $\underline{C}_6H_5$ & $CH_2\underline{C}_6H_5$), 6.16 (d, 1H, $^2J_{HH}$ = 14 Hz, C$\underline{H}_2$), 5.94 (d, 1H, $^2J_{HH}$ = 14 Hz, C$\underline{H}_2$), 3.84 (s, 3H, C$\underline{H}_3$). ^{13}C NMR (DMSO-d_6, 100 MHz, 25 ^{o}C): δ 154.2 ($\underline{C}_2N_3$), 134.5 (d, $^2J_{CP}$ = 12 Hz, P($\underline{C}_6H_5$)$_3$), 133.4 ($\underline{C}_6H_5$), 132.6 ($\underline{C}_6H_5$), 131.9 ($\underline{C}_6H_5$), 131.8 ($\underline{C}_6H_5$), 131.6 ($\underline{C}_6H_5$), 131.1 ($\underline{C}_6H_5$), 130.4 (d, $^1J_{CP}$ = 23 Hz, P($\underline{C}_6H_5$)$_3$), 129.3 ($\underline{C}_2N_3$), 129.2 ($\underline{C}_6H_5$), 128.9 (d, $^4J_{CP}$ = 9 Hz, P($\underline{C}_6H_5$)$_3$), 128.4 (d, $^3J_{CP}$ = 11 Hz, P($\underline{C}_6H_5$)$_3$), 125.9 ($\underline{C}_6H_5$), 58.9 ($\underline{C}H_2$), 38.6 ($\underline{C}H_3$). ^{31}P NMR ($CDCl_3$, 162 MHz, 25 ^{o}C): δ 25.2 ($\underline{P}Ph_3$). IR Data (KBr pellet) cm^{-1}: 3438 (s), 3053 (w), 2924 (w), 2852 (w), 1479 (w), 1433 (m), 1325 (w), 1304 (w), 1261 (w), 1236 (w), 1157 (w), 1092 (m), 1072 (w), 1020 (w), 998 (w), 771 (w), 744 (m), 699 (s), 646 (w), 530 (m), 510 (w), 494 (w). HRMS (ES): m/z 744.0265 [M-I]$^+$, calcd 744.0257. Anal. Calcd. for $C_{34}H_{30}I_2N_3PPd$•CH_3CN: C, 47.37; H, 3.64; N, 6.14. Found: C, 47.95; H, 3.46; N, 5.78.

Computational Methods

Density functional theory (DFT) calculations were performed on the metal complexes (**1-3**)**b** and (**1-3**)**c** using GAUSSIAN 09[46] suite of quantum chemical programs. The Becke three parameter exchange functional in conjunction with Lee-Yang-Parr correlation functional (B3LYP) has been employed in the study.[47, 48] The polarized basic set 6-31G(d)[49-51] was used to describe phosphorus, oxygen, nitrogen, carbon and hydrogen atoms. The Stuttgart–Dresden effective core potential (ECP) along with valence basis sets (SDD) was used for the palladium[52-56] and iodine atoms. Natural bond orbital (NBO) analysis[57] was performed using NBO 3.1 program implemented in the GAUSSIAN 09 package. Frequency calculations were performed for all the optimized structures to characterize the stationary points as minima.

The metal-ligand *donor–acceptor* interactions namely, (*i*) (*a*-NHC)−$PdI_2(NC_5H_5)$, (*ii*) (*a*-NHC)−$PdI_2(PPh_3)$ (*iii*) (*a*-NHC)PdI_2–(NC_5H_5) and (*iv*) (*a*-NHC)PdI_2–(PPh_3) were inspected by using the Charge Decomposition Analysis (CDA)[58] which is a valuable tool for analyzing the interactions between molecular fragments on a quantitative basis with an emphasis on the electron donation.[58-63] The *donor–acceptor* interaction representing the (*a*-NHC)−$PdI_2(NC_5H_5)$ interaction in (**1**−**3**)**b** and the (*a*-NHC)−$PdI_2(PPh_3)$ interaction in (**1**−**3**)**c** were examined by using this technique. The orbital interaction between a *donor a*-NHC and an *acceptor* fragment $PdI_2(NC_5H_5)$ in (**1**−**3**)**b** and a *donor a*-NHC and an *acceptor* fragment $PdI_2(PPh_3)$ in (**1**−**3**)**c** can be divided into three parts;

(i) σ-donations as given by (*a*-NHC)→$PdI_2(NC_5H_5)$ and (*a*-NHC)→$PdI_2(PPh_3)$ interactions are designated by (*d*),

(ii) π-back donations as given by (*a*-NHC)←$PdI_2(NC_5H_5)$ and (*a*-NHC)←$PdI_2(PPh_3)$ interactions designated by (*b*) and

(iii) A repulsive interaction (*r*) between the occupied FMOs of these two fragments.

Similarly, the *donor–acceptor* interactions representing the (*a*-NHC)PdI_2–(NC_5H_5) interaction in (**1**−**3**)**b** and the (*a*-NHC)PdI_2–(PPh_3) interaction in (**1**−**3**)**c**, were also examined by using this technique. The orbital interaction between a *donor* NC_5H_5 and an *acceptor* fragment (*a*-NHC)PdI_2 in (**1**−**3**)**b** and a *donor* PPh_3 and an *acceptor* fragment (*a*-NHC)PdI_2 in (**1**−**3**)**c** can also be divided into three parts;

(iv) σ-donation as given by (NC_5H_5)→PdI_2(*a*-NHC) and (Ph_3P)→PdI_2(*a*-NHC) interactions are designated by (*d*),

(v) π-back donation as given by (NC_5H_5)←PdI_2(*a*-NHC) and (Ph_3P)←PdI_2(*a*-NHC) interactions are designated by (*b*) and

(vi) A repulsive interaction (*r*) between the occupied FMOs of these two fragments.

The CDA calculations were performed using the *AOMix*[64-69] program with the B3LYP/SDD, 6-31G(d) wave function. Molecular orbital (MO) compositions and the overlap populations were calculated using the *AOMix* program. Analysis of the MO compositions in terms of occupied and unoccupied fragment orbitals (OFOs and UFOs, respectively), construction of orbital interaction diagrams, the charge decomposition analysis (CDA) were performed using the *AOMix-CDA*.[70, 71]

General procedure for the fluoride-free Hiyama cross-coupling reaction of aryl halides

In a typical catalysis run, performed in air, a 25 mL round bottom flask charged with a mixture of the aryl halides (bromides or iodides), $PhSi(OMe)_3$, NaOH and diethyleneglycol-di-*n*-butyl ether (internal standard) in the molar ratio of 1:1.2:3:1. A

palladium complex **(1–3)b** or **(1–3)c** (2 mol%) was added to the mixture followed by 6 mL solvent (dioxane/H_2O, 4:2 v/v) and the reaction mixture was heated at 80 °C for 4 hours, after which an aliquot was filtered and the product analyzed by gas chromatography using diethyleneglycol-di-*n*-butyl ether as an internal standard.

Procedure for Mercury (Hg) drop test

A 25 mL round bottom flask charged with a mixture of the aryl halides (bromides or iodides), $PhSi(OMe)_3$, NaOH and diethyleneglycol-di-*n*-butyl ether (internal standard) in the molar ratio of 1:1.2:3:1. A palladium complex **(1–3)b** or **(1–3)c** (2 mol %) and excess Hg(0) (1.00 g, 5 mmol) were added at varying time intervals and the reaction mixture was heated at 80 °C for 4 hours in 6 mL solvent (1,4-dioxane/H_2O, 4:2 v/v). The aliquots at varying time intervals and the final reaction mixture were filtered and the product analyzed by gas chromatography using diethyleneglycol-di-*n*-butyl ether as an internal standard.

Acknowledgement

We thank Department of Science and Technology (Grant No: SR/S1/IC-15/2011), New Delhi, for financial support of this research. We gratefully acknowledge Professor R. Murugavel for the use of his Single Crystal X-ray Diffraction Facility established through a DAE-SRC Outstanding Investigator Award along with the Single Crystal X-ray Diffraction Facility, Department of Chemistry IIT Bombay, India, for the crystallographic characterization data. Computational facilities from the IIT Bombay Computer Center are gratefully acknowledged. SM, MNR and MKG thank CSIR, New Delhi for research fellowship.

Supporting Information Available

Complete ref 69; the NMR, IR, mass and the CHN data of the palladium **(1–3)b** and **(1–3)c** complexes; X-ray metrical data comparison table; ORTEP plots of **2b**, **2c**, and **3b**; the B3LYP coordinates of the optimized geometries for the *cis*- and *trans*-isomers of **(1–3)b** and **(1–3)c**; NBO tables and CDA table along with orbital interaction diagrams of **(1–3)b** and **(1–3)c**. the catalysis data of control, blank, and Hg(0) drop test results; This material is available free of charge via the journal webpage.

Graphics for Table of Contents

Fluoride-free Hiyama Coupling by Palladium Abnormal N-heterocyclic Carbene Complexes

Sudipta Modak, Manoj Kumar Gangwar, Mitta Nageswar Rao, Madasu Mahesh, Alok Ch. Kalita, Vincent Dorcet, Mayuri Arun Shejale, Ray J. Butcher and Prasenjit Ghosh†*

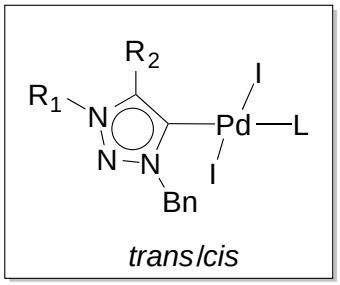

L = py, PPh_3

R_1, R_2 = Me, Et, Ph, Cy(1-OH)

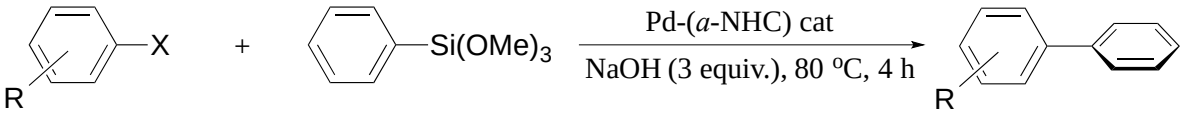

R = H, Me, $COCH_3$, NO_2

X = Br, I

A series of palladium complexes of the 1,2,3-triazole based abnormal N-heterocyclic carbene ligands of the type (*a*-NHC)PdI_2(L) [L = NC_5H_5 and PPh_3] successfully catalyzed the much convenient fluoride-free Hiyama coupling reaction in the presence of NaOH as a base in air.

References

1. H. Lebel, M. K. Janes, A. B. Charette and S. P. Nolan, *J. Am. Chem. Soc.*, 2004, **126**, 5046-5047.
2. X. Xu, B. Xu, Y. Li and S. H. Hong, *Organometallics*, 2010, **29**, 6343-6349.
3. M. Heckenroth, A. Neels, M. G. Garnier, P. Aebi, A. W. Ehlers and M. Albrecht, *Chem. Eur. J.*, 2009, **15**, 9375-9386.
4. M. Heckenroth, E. Kluser, A. Neels and M. Albrecht, *Ang. Chem. Int. Ed.*, 2007, **46**, 6293-6296.
5. R. H. Crabtree, *Coord. Chem. Rev.*, 2013, **257**, 755-766.
6. O. Schuster, L. Yang, H. G. Raubenheimer and M. Albrecht, *Chem. Rev.*, 2009, **109**, 3445-3478.
7. P. L. Arnold and S. Pearson, *Coord. Chem. Rev.*, 2007, **251**, 596-609.
8. R. Tonner, G. Heydenrych and G. Frenking, *Chem. Asian J.*, 2007, **2**, 1555-1567.
9. R. H. Crabtree, *J. Organomet. Chem.*, 2005, **690**, 5451-5457.
10. A. R. Chianese, A. Kovacevic, B. M. Zeglis, J. W. Faller and R. H. Crabtree, *Organometallics*, 2004, **23**, 2461-2468.
11. A. P. Prakasham and P. Ghosh, *Inorg. Chim. Acta*, 2015, **XX**, XXX-XXX.
12. A. Kumar and P. Ghosh, *Eur. J. Inorg. Chem.*, 2012, 3955-3969.
13. A. John and P. Ghosh, *Dalton Trans.*, 2010, **39**, 7183-7206.
14. A. John, S. Modak, M. Madasu, M. Katari and P. Ghosh, *Polyhedron*, 2013, **64**, 20-29.
15. A. John, M. M. Shaikh and P. Ghosh, *Dalton Trans.*, 2009, 10581-10591.
16. Y. Nakao and T. Hiyama, *Chem. Soc. Rev.*, 2011, **40**, 4893-4901.
17. T. Hiyama, *J. Synth. Org. Chem. Jpn.*, 2010, **68**, 729-737.
18. T. Hiyama and E. Shirakawa, *Cross-Coupling Reactions*, 2002, **219**, 61-85.
19. M. Fujita and T. Hiyama, *J. Synth. Org. Chem. Jpn.*, 1984, **42**, 293-302.
20. X. Zhang, Q. Xia and W. Chen, *Dalton Trans.*, 2009, 7045-7054.
21. J. Yang, P. Li, Y. Zhang and L. Wang, *Dalton Trans.*, 2014, **43**, 7166-7175.
22. I. Penafiel, I. M. Pastor, M. Yus, M. A. Esteruelas, M. Olivan and E. Onate, *Eur. J. Org. Chem.*, 2011, 7174-7181.
23. C. Dash, M. M. Shaikh and P. Ghosh, *Eur. J. Inorg. Chem.*, 2009, 1608-1618.
24. C. Valente, M. Pompeo, M. Sayah and M. G. Organ, *Org. Process Res. Dev.*, 2014, **18**, 559-559.
25. C. Valente, M. Pompeo, M. Sayah and M. G. Organ, *Org. Process Res. Dev.*, 2014, **18**, 180-190.
26. M. G. Organ, G. A. Chass, D.-C. Fang, A. C. Hopkinson and C. Valente, *Synthesis-Stuttgart*, 2008, 2776-2797.
27. L. Ray, M. M. Shaikh and P. Ghosh, *Dalton Trans.*, 2007, 4546-4555.
28. S. Zheng, Y. Wang, C. Zhang, J. Liu and C. Xia, *Appl. Organomet. Chem.*, 2014, **28**, 48-53.
29. C.-C. Lee, W.-C. Ke, K.-T. Chan, C.-L. Lai, C.-H. Hu and H. M. Lee, *Chem. Eur. J.*, 2007, **13**, 582-591.
30. S. K. Schneider, P. Roembke, G. R. Julius, H. G. Raubenheimer and W. A. Herrmann, *Adv. Synth. Catal.*, 2006, **348**, 1862-1873.

31. W. A. H. Sabine K. Schneider, Eberhardt Herdtweck, *J. Mol. Catal. A: Chem.*, 2006, **245**, 248–254.
32. W. A. Herrmann, V. P. W. Bo¨hm, W. K. Christian, M. G. Gsto¨ttmayr, C.-P. Reisinger and T. Weskamp, *J. Organomet. Chem.*, 2001, **617–618**, 616–628.
33. C. Valente, S. Calimsiz, K. H. Hoi, D. Mallik, M. Sayah and M. G. Organ, *Ang. Chem. Int. Ed.*, 2012, **51**, 3314-3332.
34. C. Valente, M. E. Belowich, N. Hadei and M. G. Organ, *Eur. J. Org. Chem.*, 2010, 4343-4354.
35. E. A. B. Kantchev, C. J. O'Brien and M. G. Organ, *Ang. Chem. Int. Ed.*, 2007, **46**, 2768-2813.
36. B. Cordero, V. Gomez, A. E. Platero-Prats, M. Reves, J. Echeverria, E. Cremades, F. Barragan and S. Alvarez, *Dalton Trans.*, 2008, 2832-2838.
37. R. H. Crabtree, *Chem. Rev. (Washington, DC, U. S.)*, 2012, **112**, 1536-1554.
38. M. Gorna, M. S. Szulmanowicz, A. Gniewek, W. Tylus and A. M. Trzeciak, *J. Organomet. Chem.*, 2015, **785**, 92-99.
39. M. S. Szulmanowicz, A. Gniewek, W. Gil and A. M. Trzeciak, *ChemCatChem*, 2013, **5**, 1152-1160.
40. D. Canseco-Gonzalez, A. Gniewek, M. Szulmanowicz, H. Mueller-Bunz, A. M. Trzeciak and M. Albrecht, *Chem. - Eur. J.*, 2012, **18**, 6055-6062, S6055/6051-S6055/6014.
41. S. Guo, M. H. Lim and H. Han Vinh, *Organometallics*, 2013, **32**, 7225-7233.
42. F. Alonso, Y. Moglie, G. Radivoy and M. Yus, *Eur. J. Org. Chem.*, 2010, 1875-1884.
43. P. Mathew, A. Neels and M. Albrecht, *J. Am. Chem. Soc.*, 2008, **130**, 13534-+.
44. G. M. Sheldrick, *Journal*, 1997.
45. G. M. Sheldrick, *Journal*, 1997.
46. M. J. T. Frisch, G. W.; Schlegel, H. B. Scuseria, G. E.; Robb, M. A.; Cheeseman, J. R.; Scalmani, G.; Barone, V.; Mennucci, B.; Petersson, G. A.; Nakatsuji, H.; Caricato, M.; Li, X.; Hratchian, H. P.; Izmaylov, A. F.; Bloino, J.; Zheng, G.; Sonnenberg, J. L. ; Hada, M.; Ehara, M. Toyota, K.; Fukuda, R.; Hasegawa, J.; Ishida, M.; Nakajima, T.; Honda, Y.; Kitao, O.; Nakai, H.; Vreven, T.; Montgomery, J. A.; Peralta, J. E.; Ogliaro, F.; Bearpark, M.; Heyd, J. J.; Brothers, E.; Kudin, K. N.; Staroverov, V. N.; Kobayashi, R.; Normand, J.; Raghavachari, K.; Rendell, A.; Burant, J. C.; Iyengar, S. S.; Tomasi, J.; Cossi, M.; Rega, N.; Millam, J. M.; Klene, M.; Knox, J. E.; Cross, J. B.; Bakken, V.; Adamo, C.; Jaramillo, J.; Gomperts, R.; Stratmann, R. E.; Yazyev, O.; Austin, A. J.; Cammi, R.; Pomelli, C.; Ochterski, J. W.; Martin, R. L.; Morokuma, K.; Zakrzewski, V. G.; Voth, G. A. ; Salvador, P.; Dannenberg, J. J.; Dapprich, S.; Daniels, A. D.; Farkas, O.; Foresman, J. B.; Ortiz, J. V.; Cioslowski, J.; Fox, D. J. , *Journal*, 2009.
47. A. D. Becke, *Phys. Rev. A*, 1988, **38**, 3098-3100.
48. C. T. Lee, W. T. Yang and R. G. Parr, *Phys. Rev. B*, 1988, **37**, 785-789.
49. W. J. Hehre, Ditchfie.R and J. A. Pople, *J. Chem. Phys.*, 1972, **56**, 2257-&.
50. G. A. Petersson and M. A. Allaham, *J. Chem. Phys.*, 1991, **94**, 6081-6090.
51. G. A. Petersson, A. Bennett, T. G. Tensfeldt, M. A. Allaham, W. A. Shirley and J. Mantzaris, *J. Chem. Phys.*, 1988, **89**, 2193-2218.
52. Y. Lan, C. Wang, J. R. Sowa, Jr. and Y.-D. Wu, *J. Org. Chem.*, 2010, **75**, 951-954.

53. J. Perez, A. Espinosa, J. Miguel Galiana, E. Perez, J. Luis Serrano, M. A. G. Aranda and M. Insausti, *Dalton Trans.*, 2009, 9625-9636.
54. M. R. Nimlos, C. H. Chang, C. J. Curtis, A. Miedaner, H. M. Pilath and D. L. DuBois, *Organometallics*, 2008, **27**, 2715-2722.
55. B. Goldfuss, *J. Organomet. Chem.*, 2006, **691**, 4508-4513.
56. R. Alvarez, O. N. Faza, C. S. Lopez and A. R. de Lera, *Org. Lett.*, 2006, **8**, 35-38.
57. A. E. Reed, L. A. Curtiss and F. Weinhold, *Chem. Rev.*, 1988, **88**, 899-926.
58. S. Dapprich and G. Frenking, *J. Phys. Chem.*, 1995, **99**, 9352-9362.
59. D. Nemcsok, K. Wichmann and G. Frenking, *Organometallics*, 2004, **23**, 3640-3646.
60. C. Boehme and G. Frenking, *Organometallics*, 1998, **17**, 5801-5809.
61. S. E. Vyboishchikov and G. Frenking, *Chem. Eur. J.*, 1998, **4**, 1439-1448.
62. S. F. Vyboishchikov and G. Frenking, *Chem. Eur. J.*, 1998, **4**, 1428-1438.
63. G. Frenking and U. Pidun, *J. Chem. Soc., Dalton Trans.*, 1997, 1653-1662.
64. T. Shoeib, S. I. Gorelsky, A. B. P. Lever, K. W. M. Siu and A. C. Hopkinson, *Inorg. Chim. Acta*, 2001, **315**, 236-239.
65. S. I. Gorelsky, *J. Chem. Theory Comput.*, 2012, **8**, 908-914.
66. S. I. Gorelsky and E. I. Solomon, *Theor. Chem. Acc.*, 2008, **119**, 57-67.
67. S. I. Gorelsky, *Journal*, 1997.
68. D. R. Denomme, S. M. Dumbris, I. F. D. Hyatt, K. A. Abboud, I. Ghiviriga and L. McElwee-White, *Organometallics*, 2010, **29**, 5252-5256.
69. N. Dimakis, M. Cowan, G. Hanson and E. S. Smotkin, *J. Phys. Chem. C*, 2009, **113**, 18730-18739.
70. S. I. Gorelsky, S. Ghosh and E. I. Solomon, *J. Am. Chem. Soc.*, 2006, **128**, 278-290.
71. S. I. Gorelsky, L. Basumallick, J. Vura-Weis, R. Sarangi, K. O. Hodgson, B. Hedman, K. Fujisawa and E. I. Solomon, *Inorg. Chem.*, 2005, **44**, 4947-4960.